Published in final edited form as:
Biochemistry. 2010 April 13; 49(14): 3191–3202. doi:10.1021/bi100104e.

Role of Lipid Peroxidation in Cellular Responses to D, L-Sulforaphane, A Promising Cancer Chemopreventive Agent†

Rajendra Sharma[‡,*], **Abha Sharma**[‡], **Pankaj Chaudhary**[‡], **Virginia Pearce**[§], **Rit Vatsyayan**[‡], **Shivendra V. Singh**[‖], **Sanjay Awasthi**[‡], and **Yogesh C. Awasthi**[‡]

[‡]Department of Molecular Biology and Immunology, University of North Texas Health Science Center, Fort Worth, TX

[§]Department of Pharmacology and Neuroscience, University of North Texas Health Science Center, Fort Worth, TX

[‖]Department of Pharmacology and Chemical Biology, University of Pittsburgh, Pittsburgh, PA

Abstract

D, L-Sulforaphane (SFN), a synthetic analogue of broccoli-derived L-isomer, is a highly promising cancer chemopreventive agent substantiated by inhibition of chemically-induced cancer in rodents and prevention of cancer development and distant site metastasis in transgenic mouse models of cancer. SFN is also known to inhibit growth of human cancer cells in association with cell cycle arrest and reactive oxygen species-dependent apoptosis, but the mechanism of these cellular responses to SFN exposure is not fully understood. Because 4-hydroxynonenal (4-HNE), a product of lipid peroxidation (LPO), the formation of which is regulated by hGSTA1-1, assumes a pivotal role in oxidative stress-induced signal transduction, the present study investigated its contribution in growth arrest and apoptosis induction by SFN using HL60 and K562 human leukemic cell lines as model. The SFN-induced formation of 4-HNE was suppressed in hGSTA1-1 over expressing cells, which also acquired resistance to SFN-induced cytotoxicity, cell cycle arrest, and apoptosis. While resistance to SFN-induced cell cycle arrest by ectopic expression of hGSTA1-1 was associated with changes in levels of G2/M regulatory proteins, resistance to apoptosis correlated with increased Bcl-xL/Bax ratio, inhibition of nuclear translocation of AIF, and attenuated cytochrome *c* release in cytosol. The hGSTA1-1 over expressing cells showed enhanced cytoplasmic export of Daxx, nuclear accumulation of transcription factors Nrf2 and HSF1, and up regulation of their respective client proteins, γ-GCS and HSP70. These findings not only reveal a central role of 4-HNE in cellular responses to SFN but also reaffirm that 4-HNE contributes to oxidative stress mediated signaling.

D, L-Sulforaphane (SFN), a synthetic analogue of naturally-occurring L-isomer abundant in several cruciferous vegetables (e.g., broccoli), is a potent inhibitor of chemically-induced cancer in experimental rodents (1–5). It has been shown to modulate inflammation, induce apoptosis, cause cell cycle arrest, and inhibit several Phase 1 enzymes that may activate chemical carcinogens (1). Even though the mechanisms of the chemo preventive activities of SFN are not completely understood, it has been suggested that besides inhibiting Phase I enzymes, SFN can also induce Phase 2 detoxification enzymes such as glutathione transferases (GSTs) through transcriptional activation of antioxidant response element (ARE) driven genes regulated by nuclear factor E2-related factor-2 or Nrf2 (1,6–8). Being an electrophile, SFN

†Supported in part by NIH Grants ES012171 EY 04396 (YCA), CA77495 (SA, and Supplement to this grant to AS) and CA115498 (SVS).

*Address correspondence to: Rajendra Sharma, Ph.D, Research Associate Professor, Department of Molecular Biology and Immunology, University of North Texas Health, Science Center, Fort Worth, TX 76107, Tel: 817-735-2140, Fax: 817-735-2118, rsharma@hsc.unt.edu.

causes oxidative stress by generating reactive oxygen species (ROS) which are believed to contribute to its biological properties (1). ROS mediated signaling for cell cycle arrest and apoptosis along with DNA damage and depleted cellular glutathione (GSH) levels are also implicated in the mechanisms of its chemopreventive activity (1–8).

Membrane lipid peroxidation (LPO) is an inevitable consequence of ROS induced oxidative stress and there is ample evidence that the electrophilic LPO products including lipid hydroperoxides and α β-unsaturated carbonyls particularly, 4-hydroxynonenal (4-HNE) play a crucial role in ROS induced signaling (9–17). In recent years, 4-HNE has emerged as an important second messenger molecule involved in signaling for cell proliferation, cell cycle arrest, differentiation, apoptosis, and regulation of the expression of a multitude of genes in cells of diverse origin (9–13). 4-HNE has also been shown to modulate survival and death signaling pathways in a concentration dependent manner by interacting with several signaling proteins involved in both, the extrinsic and the intrinsic pathways of apoptosis (18,19). Furthermore, 4-HNE has been shown to modulate the expression and functions of stress-responsive transcription factors, Nrf2 (20) and heat shock factor1 (HSF1), and the transcription repressor, Daxx or death associated Fas interacting protein (19,21,22).

Since ROS are implicated in the biological activities of SFN we reasoned that ROS induced LPO products, particularly 4-HNE could contribute to these activities. We have tested this postulate by studying the effects of SFN in an *in vitro* model in which ROS induced LPO has been suppressed by over expression of the alpha class GSTA1-1 isozyme. Apart from catalyzing the conjugation of toxic electrophiles to GSH, GST A1-1 also catalyzes the GSH-dependent reduction of phospholipids hydroperoxides (PL-OOH) and fatty acid hydroperoxides (FA-OOH) through its Se-independent glutathione peroxidase (GPx) activity thereby terminating the autocatalytic chain of LPO reactions resulting in decreased intracellular 4-HNE levels (14,15,23). Previous studies conducted on various GSTA1-1 transfected cell types in culture have shown that these cells have reduced 4-HNE levels and acquire resistance to ROS induced apoptosis (9,10,23). Present studies were designed to elucidate the putative contributions of 4-HNE in the mechanisms of SFN-induced cytotoxicity and signaling in two human leukemic cell lines viz. HL60 derived from a promyelocytic leukemia patient, and K562, originated from chronic myelogenous leukemia having specific chromosome abnormality designated as Philadelphia chromosome(24). Specifically, we have addressed the question as to whether or not the over expression of hGSTA1-1 can affect SFN-induced cytotoxicity and signaling events by modulating intracellular levels of 4-HNE in these cells. We have also studied the effects of SFN on cell cycle arrest and apoptosis related proteins, stress responsive transcription factors Nrf2, HSF1, and the transcription repressor Daxx. Furthermore, we have examined whether or not these effects of SFN can be abrogated by the over expression of GSTA1-1 in these cells. Results of these studies strongly indicate that 4-HNE plays a crucial role in the mechanisms of SFN-induced signaling. Our data also suggests that the α-class GSTs can modulate cell survival and death signaling by regulating the intracellular concentrations of 4-HNE which reinforces our previous assertion that these enzymes play an important role in the over all regulation of ROS induced signaling.

Materials and Methods

Materials

Epoxy-activated Sepharose 6B, glutathione (GSH), 1-chloro-2, 4-dinitrobenzene (CDNB), cumene hydroperoxide (CU-OOH), and 3-(4, 5-dimethylthiazol-2-yl)-2, 5-diphenyltetrazolium bromide (MTT) were obtained from Sigma (St. Louis, MO). RPMI 1640 medium, fetal bovine serum, phosphate-buffered saline (PBS), and penicillin/streptomycin were purchased from GIBCO, Inc (Grand Island, NY). All reagents for SDS polyacrylamide

gel electrophoresis (SDS-PAGE) and Western transfer were purchased from Invitrogen (Carlsbad, CA). Sulforaphane (SFN) was obtained from Sigma (St. Louis, MO).

Antibodies

Antibodies against Bax (N-20, sc-493, polyclonal), caspase3 (sc-7148, polyclonal), Bcl-xL (sc-23958, monoclonal), Nrf2 (sc-722, polyclonal), Daxx (sc-7152, polyclonal), and HSF1(sc-9144, polyclonal), Hsp 70, cyclin B1 (sc-595), cdk1/cdk2 (sc-53219), histone 3(sc-H0164, polyclonal), and VDAC1 (sc-8829, polyclonal) were obtained from Santa Cruz Biotechnology (Santa Cruz, CA) while AIF (# 4642, polyclonal) was obtained from Cell Signaling Technology, Inc. Horseradish peroxidase (HRP)-conjugated secondary antibodies as well those against GAPDH were purchased from Southern Biotech (Birmingham, AL). Polyclonal antibodies raised against the human α class GSTs and the GPx were the same as those used in our previous studies (15). Antibodies against 4-HNE-protein adduct (4-HNE 11S) were purchased from Alpha Diagnostics (San Antonio, TX).

Cell Cultures

HL60, and K562 cells were grown as suspension cultures in RPMI 1640 medium containing L-glutamine supplemented with 10% (v/v) fetal bovine serum and 1% penicillin/streptomycin (v/v) at 37°C in a 5% CO_2 humidified atmosphere. Cells were passaged by mechanical de-segregation and transfer of small number of cells to new flasks.

Stable transfection with hGSTA1

Based on the previously reported cDNA sequence for *h*GS*TA1* (23), PCR primers were designed to amplify the complete coding sequence (656 base pair) of *hGSTA1* from pET-30a (+)/hGST*A1* vector. The amplified cDNA was sub cloned into the pTarget-T mammalian expression vector (Promega). Cells were then transfected with pTarget-T/*hGSTA1*, or with the vector alone, using the Lipofectamine Plus reagent (Invitrogen, San Diego, CA) according to the manufacturer's instructions. Stable transfectants were isolated by selection on 300μg/ml G418 for ~2 weeks. Single clones of stably transfected cells were obtained by limiting dilution. Further characterization of the selected G418- resistant stable clones expressing hGSTA1-1 was achieved by Western blotting and enzyme assays.

Enzyme assays

For determination of the activity of the antioxidant enzymes and the enzymes involved in GSH homeostasis in the pTarget-T/*hGSTA1* or the empty vector transfected cells, the respective cells were homogenized in buffer A containing 1.4mM β-mercaptoethanol (β-Me) by sonication. The sonicated cells were centrifuged for 45 min at 28,000g at 4°C, and the 28,000g supernatant was then subjected to GSH-affinity chromatography (25). The purified hGSTA1-1 was eluted from the GSH-affinity resin in 50mM Tris-HCl, pH 9.6 containing 10mM GSH and 1.4 mM β-Me. Enzyme activities were assayed both in the crude 28,000g fraction as well as the purified hGSTA1-1.

GST activity towards CDNB (26) and SFN (27), GPx activity towards cumene hydroperoxide (CU-OOH) (28), and the activities of glutathione reductase (GR) and γ-glutamylcysteine synthetase (γ-GCS) were determined by the previously reported methods (29,30).

Western Blot Analysis

For the detection of the expressed hGSTA1-1 protein, stably transfected HL60 and K562 cells were collected by centrifuging for 5 min at 500g, washed twice with PBS, and resuspended in hypotonic lysis buffer (buffer A). After a brief sonication for 15 sec, three times each, the cell lysate was centrifuged at 28,000g and the supernatants were measured for protein concentration

by the Bradford method (31). Cell lysates containing 50μg protein were separated with 12% polyacrylamide gels according to the method of Laemmli (32), and subjected to Western blot analysis essentially according to the method of Towbin et al. (33) using the polyclonal antibodies against the human alpha class GSTs. Chemiluminescence reagents (Invitrogen) were used to develop the immunoblots by following the manufacturer's instructions.

For detection of other proteins, treated cells were collected, washed with PBS and resuspended in radio-immunoprecipitation assay (RIPA) lysis buffer, containing 1x PBS, (pH 7.4), 1% Nonidet-P-40 (NP-40), 0.5% sodium deoxycholate, 0.1% sodium dodecyl sulphate, 1mM phenylmethanesulfonyl fluoride (PMSF), and 2μg/ml of pepstatin. After sonicating three times for 5s, the lysates were centrifuged at 14,000 rpm for 15 min and the supernatants collected. Sub-cellular fractionated extracts containing cytoplasmic, mitochondrial and nuclear proteins were prepared by a modification of the published procedure used previously (34). Protein concentrations in various extracts were determined by the Bradford assay (31). Separation of proteins in the various extracts was ascertained by Western blot analysis using marker antibodies for different proteins as described above.

Cytotoxicity Assays

The sensitivity of the cells to SFN was measured by the MTT assay as described by Mosmann (35) with slight modifications. Briefly, 2×10^{4} cells in 190 μl of medium were plated to each well in 96-well flat bottomed micro titer plates. 10μl of PBS containing various amounts of SFN were added. Eight replicate wells for each concentration of SFN were used in these experiments. Following incubation of the plates at 37°C for 24h, 10μl of MTT solution (5mg/ml in PBS) was added to each well, and the plates were incubated for additional 4h at 37°C. The plates were centrifuged at 2000g for 10 min. The medium within the wells was aspirated and 100μl of dimethylsulfoxide (DMSO) was added to each well. The intracellular formazan dye crystals were dissolved by shaking the plates at room temperature for 2h. The absorbance of formazan at 562nm was measured using a microplate reader (Elx808 BioTek Instruments, Inc). The concentration of SFN resulting in a 50% decrease in formazan formation (IC_{50}) was obtained by plotting a dose-response curve.

Determination of cellular GSH levels

Intracellular GSH content was determined in cellular homogenates prepared in Buffer A without β-mercaptoethanol by the method of Beutler et al (36). Briefly, cells were resuspended in buffer A and sonicated. To 200μl of the lysate, 300 μl of precipitating solution (0.2 M glacial meta-phosphoric acid, 5 M NaCl, 5 mM EDTA) was added. The acid-precipitated proteins were pelleted by centrifugation at 4°C for 10 min at 20, 000 × g. To determine the GSH content, 200 μl of the acid-soluble supernatants were mixed with 800 μl of 0.3 M Na_2HPO_4, mixed and the initial OD read at 412nm. 100 μl of 0.6 mM 5, 5-dithiobis (2-nitrobenzoic acid) (DTNB in 1% sodium citrate) was added to a final volume of 1 ml. The increase in absorption at 412 nm was monitored and used to determine the amount of GSH in the samples.

Determination of the intracellular 4-HNE levels

Intracellular levels of 4-HNE in the control and SFN (20μM) treated cells (2×10^{7}) were determined spectrophotometrically by using the LPO 586 (Oxis International) measurement kit as per the manufacturer's instructions.

Immunofluorescence detection of 4-HNE-protein adducts and localization of Nrf2

Control and SFN-treated HL60 cells were washed 2x with ice-cold phosphate buffered saline (PBS) (pH 7.4). These cells were spread onto clean glass slides, using a cytospin (Cytospin 2, Shandon, USA), fixed with 4% paraformaldehyde for 30 min at room temperature and

permeabilized with 0.1% Triton X-100 for 30 min. Slides were once again washed with PBS and blocked with 3% goat serum in PBS for 2h. For the immunofluorescence detection of 4-HNE adducts, cells were incubated with primary antibodies (1: 250) against the 4-HNE-protein adduct overnight at 4°C in a humidified chamber. After washing them 3× 10 min with PBS, cells were incubated with TRITC conjugated anti-mouse secondary antibodies (1:1000) for 2h. Slides were mounted in a medium containing 1.5 μg/ml DAPI(Vector Laboratories, Inc., USA) and observed under the fluorescence microscope (Olympus, Japan). For the immunofluorescence detection of Nrf2, control and SFN-treated cells were processed in a similar manner as described above except that these cells were incubated with anti-Nrf2 antibody diluted 1:50 in PBS containing 1% bovine serum albumin overnight at 4 °C. After washing with ice-cold PBS, the slides were incubated with FITC-labeled goat anti-rabbit immunoglobulin G (1:100; Southern Biotech, USA) for 2h at room temperature. The slides were viewed under a Nikon E600 microscope with 40X objective using filters for DAPI, FITC and TRITC stains.

Flow cytometric analysis

The effect of SFN on cell cycle distribution was determined by FACS analysis according to the protocol provided by Flow Cytometry & Laser Capture Microdissection Core Facility, UNTHSC. Cells (2×10^5 in a 100mm dish) were treated with 20μM SFN for 5 and 24h at 37° C. Appropriate controls were also set up. Care was taken to assure that the cells were no more than 50% confluent on the day of the treatment. After treatment, floating and adherent cells were collected, washed with PBS two times by centrifugation at 300g for 5 min at 4°C, and fixed with 70% ethanol. On the day of flow analysis, cell suspensions were centrifuged, counted and approximately 600,000 cells were resuspended in 500 μl PBS in flow cytometry tubes. Cells were incubated with 2.5 μl RNAse (20mg/ml) and incubated at 37°C for 30 min after which they were treated with 5 μl of propidium iodide (1mg/ml) solution and incubated at room temperature for 30 min in the dark. The stained cells were analysed using the Beckman Coulter Cytomics FC500, Flow Cytometry Analyzer. CXP2.2 analysis software from Beckman Coulter was used to deconvolute the cellular DNA content histograms to obtain quantitation of the percentage of cells in the respective phases (G1, S and G2/M) of the cell cycle. Appearance of the sub-G0/G1 peak indicates the cells undergoing apoptosis.

Statistical analysis

Data presented are mean ±SD of triplicate samples from three different experiments. Statistical significance between different groups was determined using Students t test. A p value of <0.05 was considered significant.

Results

Stable transfection of hGSTA1 in HL60 and K562 cells

The cells were separately transfected with pTarget empty vector, and the pTarget-T/*hGSTA1* cDNA. Subsequent selection of stably transfected clones in the presence of G418 resulted in high expression of hGSTA1-1 as indicated by the results of Western blot analysis shown in Fig 1A and B where the *hGSTA1* transfected cells showed a robust expression of hGSTA1-1 while the wild type and empty vector-transfected cells did not show any detectable expression of hGSTA1-1. There were no noticeable differences in the morphology or growth kinetics of the empty vector, and *hGSTA1*-transfected cells.

GST activity towards 1-chloro-2, 4-dinitrobenzene (CDNB) was found to be increased by almost 2-fold in *hGSTA1*-transfected cells whereas selenium-independent GPx activities towards cumene hydroperoxide (CU-OOH) in *h*GST*A1*-transfected cells was increased by about 4.5-fold as compared to that in empty vector-transfected cells. Lesser fold increase in

the conjugating activity against CDNB is perhaps because of the high constitutive level of this activity in cells (Table 1). Together, these results confirmed the presence of a functional hGSTA1-1 protein in the transfected cells. Similar to that observed in our previous studies (16,17), the activities of catalase, superoxide dismutase, and GPx activity towards H_2O_2 were comparable in the vector and *GSTA1* transfected cells. Since GSTA1-1 has no GPx activity towards H_2O_2, these results indicated that the capacities of the empty vector or the *GSTA1* transfected cells to detoxify H_2O_2 and superoxide were similar. There was a 2-fold increase in the activity of gamma glutamyl cysteine synthase (γ-GCS), the rate limiting GSH synthesizing enzyme. There was a slight but statistically insignificant increase in the GSH levels of hGSTA1-1 expressing cells. However, depletion of GSH levels upon SFN treatment was found to be comparable in the vector and *hGSTA1* transfected cells(data not presented) indicating that intracellular alterations in GSH levels did not contribute to the effects of *GSTA1*-transfection on SFN cytotoxicity, and SFN-mediated signaling described later in this communication.

Overexpression of hGSTA1-1 inhibits SFN-induced LPO

In order to assess the effect of *GSTA1* transfection on SFN-induced LPO, we compared the levels of 4-HNE in empty vector and *hGSTA1* transfected cells spectrophotometrically as well as by comparing the immunofluorescence using antibodies against 4-HNE. Results of these studies showed that SFN treatment caused a dose dependent increase in cellular 4-HNE levels and that the expression of hGSTA1-1 attenuated both, the basal and SFN-induced 4-HNE levels in these cells (Fig. 1C and 1D). Overall, our studies indicated that the over expression of hGSTA1-1 in cells significantly suppressed the generation of 4-HNE and the accumulation of 4-HNE-protein adducts.

Overexpression of hGSTA1-1 attenuates SFN cytotoxicity

To investigate the protective role of hGSTA1-1 against SFN cytotoxicity in HL60 and K562 cells, we compared the effects of SFN at different concentrations in the empty vector, and *hGSTA1*-transfected HL60 cells for a period of 24h by MTT assay. The IC_{50} values of SFN as determined in three independent experiments were found to be 19± 3.4, and 42 ±2.6 μM for the empty vector and hGSTA1-1 overexpressing HL60 cells, respectively whereas the IC50 of SFN for empty vector and hGSTA1-1 overexpressing K562 cells were found to be 16.4 ± 1.64 and 39.5 ± 2.23 μM respectively. The cell viability data presented in Fig. 2A and 2B indicated that the expression of hGSTA1-1 in the transfected cells conferred about 2-fold resistance to SFN-induced cytotoxicity.

Over expression of hGSTA1-1 attenuates SFN-induced cell cycle arrest

A number of studies have shown that plant derived isothiocyanates such as SFN exert their cytotoxicity on cancer cells through cell cycle arrest in the G2/M phase and apoptosis (2–5). These effects have been attributed to ROS induced signaling. Since transfection with *hGSTA1* was observed to attenuate intracellular 4-HNE levels (Fig. 1C), we examined if hGSTA1-1 over expressing cells were resistant to SFN-induced cell cycle arrest. For these experiments we treated the empty vector and *hGSTA1*-transfected cells with 20μM SFN for various time points and quantified percent cells in the different phases of cell cycle in the control and SFN-treated cells by flow cytometry. Microscopic observations supported by the FACS analysis data (Fig 3 A–E) demonstrated that SFN (20μM) caused a gradual time-dependent accumulation of the empty vector and *h*GST*A1*-transfected cells in the G2/M phase of the cell cycle. Vector transfected cells however were significantly more susceptible to the SFN-induced cell cycle arrest in the G2/M phase and subsequent apoptosis (subG0/G1 cells) as compared to those expressing hGSTA1-1 (Fig. 3, C–E). A significant population of cells underwent apoptosis upon exposure to SFN (Fig. 3B–E) and this population of apoptotic cells

was significantly attenuated in *hGSTA1*-transfected cells. When empty vector and *GSTA1*-transfected cells were allowed to recover for 24h after SFN treatment in medium without SFN, a significantly higher percentage (~ 30%) of hGSTA1-1 over expressing cells recovered from SFN-induced G2/M cell cycle arrest as compared (~16%) to those transfected with the empty vector (Fig. 3, B–E). During 24h recovery period, percentage of apoptotic cells in empty vector (VT) transfected cells was significantly higher as compared to those expressing hGSTA1-1. Considering that the primary ROS detoxifying enzymes, catalase and SOD were comparable in vector and *hGSTA1* transfected HL60 cells and that the GSTA1-1 does not express GPx activity towards H_2O_2, these results strongly indicated that the SFN-induced accumulation of 4-HNE contributed to the cell cycle arrest of these cells and that over expression of hGSTA1-1 rescued them from G2/M cell cycle arrest by limiting SFN-induced formation of 4-HNE.

Overexpression of hGSTA1-1 affects proteins involved in SFN-induced cell cycle arrest

Cell cycle progression is regulated by three classes of proteins viz., cyclins, cyclin-dependent kinases (cdks), and cdk inhibitors (CKIs). During growth arrest, an increase in the levels of CKIs is reported along with a reduction in the levels of cyclins (37,38). An increase in cdk1-cyclin B1 complex is reported during the entry of cells into mitosis. Our results (Fig.3F and 3G) showing significantly higher expression of cyclin B1 and Cdk1 (cdc2) in hGSTA1-1 over expressing cells as compared to the empty vector transfected cells are consistent with the observed higher rate of recovery of GSTA1-1 over expressing cells from SFN-induced cell cycle arrest. These results implicate intracellular level of 4-HNE as a major determinant of cell cycle arrest and suggest that *GSTA1* transfection provides protection from SFN-induced cell cycle arrest.

Over expression of hGSTA1-1 affects the apoptotic proteins, Bcl-xL and Bax

Previous studies have shown that cells respond to various physico-chemical stressors rapidly by modulating different pro-and anti-apoptotic components of the signaling machinery (10, 15,16–19). Moreover, as described in the preceding section, results of FACS analysis showed that the exposure of cells to SFN induces G2/M cell cycle arrest of HL60 cells with in a period of 5h. Therefore, the effects of SFN on pro and anti-apoptotic signaling proteins in both these cell types were analyzed after 0.5-5h treatment. Bcl-xL is an anti-apoptotic BH-3 only family of proteins (39) which is known to directly interact with the pro-apoptotic protein Bax to prevent its translocation to mitochondria thereby inhibiting apoptosis (40). Results presented in Fig. 4 A indicated that a significantly higher expression of Bcl-xL was observed in SFN-treated hGSTA1-1 over expressing cells as compared to those transfected with empty vector. Our results also showed (Fig. 4B) the inhibition of mitochondrial translocation of Bax and the release of cytochrome C into cytosol (Fig. 4C) in hGSTA1-1 over expressing cells. These results are consistent with the observed resistance of GSTA1-1 over expressing cells to SFN-induced apoptosis. Taken together, these results strongly suggest a crucial role of the LPO product, most likely 4-HNE in SFN induced signaling for cell cycle arrest and apoptosis.

SFN- induced nuclear accumulation of AIF is inhibited in hGSTA1-1over expressing cells

Apoptosis inducing factor (AIF) is a bifunctional NADH oxidase involved in mitochondrial respiration and caspase independent apoptosis (41,42). AIF plays a pro-survival role through its redox activity in mitochondria, but assumes a lethal function upon being translocated to the nucleus where it causes partial chromatin condensation and DNA fragmentation (42). We therefore compared any possible effect of SFN on AIF in the vector and *hGSTA1*-transfected cells. Results of these experiments (Fig. 4D) showed that while in the vector transfected cells, SFN promoted a time dependent increase in nuclear accumulation of AIF, this effect of SFN was almost completely abrogated in hGSTA1-1 over expressing cells. Bax is reported to facilitate the nuclear accumulation of AIF (40). Relatively higher accumulation of Bax in the

mitochondria of vector transfected cells upon SFN treatment was consistent with the observed higher nuclear accumulation of AIF in these cells (Fig. 4 B and D). This would also be consistent with the observed higher sensitivity of the vector transfected cells to SFN-induced apoptosis as compared to the hGSTA1-1 over expressing cells. Strikingly, lack of any significant induction of caspase3 during SFN-induced apoptosis suggested that caspase3 independent apoptosis in these cells may be mediated by AIF which was attenuated in *hGSTA1*-transfected cells with ameliorated 4-HNE levels.

SFN- induced nuclear accumulation of Nrf2 is exacerbated in hGSTA1-1 over expressing cells

The transcription factor Nrf2 interacts with ARE and regulates the transcription of genes encoding antioxidant proteins (6,7,43) involved in protection against oxidative stress. We compared the levels of Nrf2 in the cytosolic and nuclear fractions of SFN treated empty vector and *hGSTA1* transfected cells to study the possible role of 4-HNE in the nuclear translocation of Nrf2 upon SFN treatment. Results of these studies (Fig. 5A–C) indicated that exposure to SFN led to an enhanced accumulation of Nrf2 in the nuclear extracts of both, the empty vector and *hGSTA1* transfected cells in a time- dependent manner. Western blot analyses data (Fig. 5A) indicated a rapid nuclear accumulation of Nrf2 within 30 min of SFN treatment which persisted for at least up to 5h thereby suggesting this to be an early event for the increased transcription of antioxidant enzymes to protect cells from the SFN-induced oxidative stress. The results of Western blot analysis and immunofluorescence studies clearly showed that the nuclear accumulation of Nrf2 was significantly higher in *hGSTA1* transfected cells (Fig.5A–C). Nuclear translocation of Nrf2 has been suggested to be initiated by its dissociation from Keap1 during oxidative stress (44). Our results showing relatively higher nuclear accumulation of Nrf2 in 4-HNE depleted, hGSTA1-1 over expressing cells suggested that SFN-induced up regulation of Nrf2 is independent of 4-HNE or lipid peroxidation and may result from the direct interaction of electrophilic SFN with the cysteine residues of Keap1.

Overexpression of hGSTA1-1 exacerbates SFN- induced activation of HSF1 by promoting translocation of Daxx to the cytosol

The role of transcription factor HSF1 has been suggested in the mechanisms of defense against oxidative stress (45). Heat shock proteins (Hsps), the client proteins of HSF1, play an important role in the recovery of cells from the toxic effects of oxidative stress caused by heat, radiation and chemicals (19–21,45,46). Western blot data presented in Fig.6A and 6B indicated significantly more induction and enhanced nuclear accumulation of HSF1 in SFN-treated hGSTA1-1 over expressing HL60 and K562 cells respectively as compared to that in vector transfected cells. This correlated with significantly higher expression of Hsp70 (Fig. 6C) in the *hGSTA1* transfected cells as compared to the vector transfected cells. Death associated Fas binding protein, Daxx has been shown to be a transcription repressor which translocates to cytoplasm upon exposure of cells to oxidative stress (19,47). The translocation of Daxx from nucleus to cytoplasm has been shown to induce nuclear accumulation of HSF1 and induction of Hsp70 (19). Results presented in Fig. 6D and 6E show that a time dependent accumulation of Daxx in the cytoplasm of *hGSTA1*-transfected cells is accompanied with HSF1 activation These effects of SFN on HSF1 and Daxx appear to be independent of 4-HNE. Taken together, our results suggest that GSTA1-1 may also protect cells from SFN-induced toxicity through the activation of stress responsive HSF1 and Daxx.

Discussion

It has already been well demonstrated that exposure to SFN causes the generation of ROS in cells and tissues. Furthermore, ROS-induced cellular signaling is believed to contribute to at least some of its known chemo-preventive properties (1–5). The results of present studies

indicate that at least some of the biological activities associated with the chemo-protective properties of SFN may be mediated through LPO-products, particularly 4-HNE generated during SFN-induced oxidative stress and that these activities can be modulated by GSTs. Over expression of GSTA1-1 in HL60 and K562 cells was observed to suppress 4-HNE levels by limiting SFN- induced LPO and confer a remarkable resistance to cells against SFN-mediated cytotoxicity, cell-cycle arrest, and apoptosis. These findings are consistent with recent studies (9) showing that 4-HNE is involved in the mechanisms of ROS mediated signaling and that GSTs play an important regulatory role in oxidative stress-induced signaling.

The attenuation of 4-HNE levels in hGSTA1-1 over expressing cells after SFN treatment underscores the role of GSTA1-1 in regulating the levels of 4-HNE. Since 4-HNE is known to cause cell cycle arrest, apoptosis, and cytotoxicity to cells via necrosis (48–50), the observed effects of GSTA1-1 over expression on these biological activities of SFN may be attributed to the LPO suppression capability of GSTA1-1. While it is possible that increased SFN-conjugating activity of GSTA1-1 over expressing cells may lower the actual concentration of SFN by its accelerated conjugation with GSH, our results showing no significant alteration in the GSH levels of SFN treated empty vector, or *hGSTA1*-transfected cells suggest that the observed protective effects of GSTA1-1 against SFN toxicity may be imparted preferentially through the inhibition of SFN induced LPO and consequent lowering of 4-HNE levels, rather than GST-GSH mediated detoxification of SFN.

The observed effects of SFN in HL60 and K562 cells are essentially similar to those reported in previous studies with colon and prostate cancer cells (2,3). Exposure to SFN caused cell cycle arrest in the G2/M phase in both these cell types. hGSTA1-1 over expression caused approximately two-fold resistance to SFN-induced cell cycle arrest as well as apoptosis. Cell cycle arrest at the G2/M phase by SFN has been suggested to be regulated by cell cycle related proteins, cyclin B1 and Cdk1, and /or disruption of normal mitotic microtubule polymerization and histone acetylation (51,52). Cyclins and cyclin-dependent kinase complexes play an important role in the G2-M transition mechanisms. By binding to Cdk1/2, cyclin B1 can activate Cdk1/2 (cdc2) to facilitate its nuclear accumulation for mitotic initiation in the late G2 phase of mammalian cells (4,37,38). A time dependent induction of Cdk1 and cyclin B1 in SFN-treated hGSTA1-1 over expressing cells indicate that the inhibition of SFN-induced accumulation of 4-HNE by hGSTA1-1 rescued them from the G2/M arrest through an up-regulated expression of Cdk1 and cyclin B1. Inhibition of SFN induced apoptosis in GSTA1-1 over expressing cells could also be attributed to the effect of suppression of 4-HNE levels and subsequent modulation of mitochondrial apoptotic pathways. This is indicated by the activation of Bcl-xL and attenuated translocation of Bax to mitochondria in *GSTA1*-transfected cells. Furthermore, in *GSTA1*-transfected cells, SFN-induced cytochrome C release to cytosol and nuclear accumulation of AIF are also inhibited. These findings would indicate that SFN can induce apoptosis in human erythroleukemic cells through mitochondria mediated caspase independent pathway (53) and that this can be modulated by suppression of LPO by GSTs.

Transcriptional regulation of many genes encoding antioxidant proteins under stressful conditions for maintenance of cellular redox homeostasis involves an important role for Nrf2, a short half life protein, sequestered in the cytoplasm through its binding with Keap1. Nrf2 is targeted for ubiquitination when bound to its inhibitory protein Keap1, but is activated by oxidative stress when it dissociates from Keap1, translocates into the nucleus, and transactivates the antioxidant response element (ARE) to induce the phase 2 detoxification, and antioxidant enzymes (1,6–8). Our results of Western analysis and immunfluorescence microscopy showed nuclear accumulation of Nrf2 upon SFN exposure, in the nuclei of both, the empty vector, and *hGSTA1*-transfected cells. However, relatively higher nuclear accumulation of Nrf2 observed in hGSTA1-1 over expressing cells as compared to the empty vector transfected cells may be a contributory factor to the resistance of GSTA1-1 over

expressing cells to SFN toxicity. Enhanced nuclear accumulation of Nrf2 in GSTA1-1 over expressing cells upon treatment with SFN may also suggest a reprogramming of protective machinery of the cells to alleviate electrophilic stress. Our results demonstrate that SFN exposure leads to nuclear translocation of HSF1 and up regulated expression of a representative HSF1-client protein, Hsp70 which correlates with the observed inhibition of SFN- induced nuclear accumulation of AIF in GSTA1-1 over expressing cells and their resistance to apoptosis. Our results also suggest that SFN-induced up regulation of heat shock proteins most likely results from the translocation of HSF1 transcription repressor protein- Daxx (19) from the nucleus to cytoplasm. We demonstrate that SFN-treatment promotes the translocation of Daxx from nucleus to cytoplasm which is accompanied with the nuclear translocation of HSF1 and up regulation of the expression of HSF1 related genes. These combined effects of GSTA1-1 should collectively contribute to the protective mechanisms against oxidative stress caused by SFN. Interestingly, these results suggest that similar to 4-HNE (19), SFN also induces mechanisms to self limit its own toxicity. Since GSTA1-1 over expressing cells with sub-constitutive 4-HNE levels show higher degree of activation of Nrf2 and HSF1, it appears unlikely that 4-HNE is involved in up regulation of these parameters. Instead, SFN being a strong electrophilic compound can directly interact with Keap1 and Daxx to affect the activation of Nrf2 and HSF1, respectively.

In summary, the results of the present studies indicate that SFN-induced LPO contributes to its cytotoxicity to cells which can be inhibited by the over expression of GSTA1-1 and that the protective effects of GSTA1-1 are associated with its ability to regulate 4-HNE levels in cells. GSTA1-1 and possibly other Alpha class GSTs seem to play a crucial role in protecting cells from the cell-cycle arrest and apoptotic effects of SFN through a well orchestrated interplay of several pro-survival signaling pathways as presented in a model shown in Fig. 7. Perhaps this model can be extrapolated to the overall protective role of GSTs during oxidative/electrophilic stress and the role of 4-HNE in regulation of signaling. Further studies are needed to validate this model, particularly for deciphering the mechanisms of interplay between Nrf2 and HSF1 and associated genes upon exposure to agents that promote LPO.

Abbreviations

SFN	D, L sulforaphane
4-HNE	4-hydroxynonenal
GST	glutathione transferase
hGSTA1-1	human glutathione transferase isozyme A1-1
LPO	lipid peroxidation
ROS	reactive oxygen species
GSH	glutathione
Daxx	death associated Fas binding protein
Nrf2	Nuclear factor-E2-related factor-2
HSF1	heat shock factor 1
CDNB	1-chloro-2.4-dinitrobenzene
FACS	Fluorescence activated cell sorting

Acknowledgments

We thank Xiangle Sun (Core Facility at the University Of North Texas Health Science Center, Fort Worth, TX) for helping with flow cytometry and laser capture micro-dissection (supported by National Institutes of Health Grant ISIORR018999-01A1).

References

1. Juge N, Mithen RF, Traka M. Molecular basis for chemoprevention by sulforaphane: a comprehensive review. Cell Mol. Life Sci 2007;64:1105–1127. [PubMed: 17396224]
2. Payrastre GL, Li P, Lumeau S, Cassar G, Dupont MA, Chevolleau S, Gasc N, Tulliez J, Tercé F. Sulforaphane, a naturally occurring isothiocyanate, induces cell cycle arrest and apoptosis in HT29 human colon cancer cells. Cancer Res 2000;60:1426–1433. [PubMed: 10728709]
3. Singh SV, Herman-Antosiewicz A, Singh AV, Lew KL, Srivastava SK, Kamath R, Brown KD, Zhang L, Baskaran R. Sulforaphane-induced G2/M phase cell cycle arrest involves checkpoint kinase 2-mediated phosphorylation of cell division cycle 25C. J Biol Chem 2004;279:25813–25822. [PubMed: 15073169]
4. Singh SV, Srivastava SK, Choi S, Lew KL, Antosiewicz J, Xiao D, Zeng Y, Watkins SC, Johnson CS, Trump DL, Lee YJ, Xiao H, Herman-Antosiewicz A. Sulforaphane-induced cell death in human prostate cancer cells is initiated by reactive oxygen species. J. Biol. Chem 2005;280:19911–19924. [PubMed: 15764812]
5. Xiao D, Srivastava SK, Lew KL, Zeng Y, Hershberger P, Johnson CS, Trump DL, Singh SV. Allyl isothiocyanate, a constituent of cruciferous vegetables, inhibits proliferation of human prostate cancer cells by causing G2/M arrest and inducing apoptosis. Carcinogenesis 2003;24:891–897. [PubMed: 12771033]
6. McWalter GK, Higgins LG, McLellan LI, Henderson CJ, Song L, Thornalley PJ, Itoh K, Yamamoto M, Hayes JD. Transcription factor Nrf2 is essential for induction of NAD(P)H:quinone oxidoreductase 1, glutathione S-transferases, and glutamate cysteine ligase by broccoli seeds and isothiocyanates. J. Nutr 2004;134:3499S–3506S. [PubMed: 15570060]
7. Zhang Y. Cancer-preventive isothiocyanates: measurement of human exposure and mechanism of action. Mutat. Res 2004;555:173–190. [PubMed: 15476859]
8. Thimmulappa RK, Mai KH, Srisuma S, Kensler TW, Yamamoto M, Biswal S. Identification of Nrf2-regulated genes induced by the chemopreventive agent sulforaphane by oligonucleotide microarray. Cancer Res 2002;62:5196–5203. [PubMed: 12234984]
9. Yang Y, Sharma R, Sharma A, Awasthi S, Awasthi YC. Lipid peroxidation and cell cycle signaling: 4-hydroxynonenal, a key molecule in stress mediated signaling. Acta Biochim Pol 2003;50:319–336. [PubMed: 12833161]
10. Cheng JZ, Singhal SS, Sharma A, Saini M, Yang Y, Awasthi S, Zimniak P, Awasthi YC. Transfection of mGSTA4 in HL-60 cells protects against 4-hydroxynonenal-induced apoptosis by inhibiting JNK-mediated signaling. Arch Biochem Biophys 2001;392:197–207. [PubMed: 11488593]
11. Cheng JZ, Singhal SS, Saini M, Singhal J, Piper JT, Van Kuijk FJ, Zimniak P, Awasthi YC, Awasthi S. Effects of mGST A4 transfection on 4-hydroxynonenal-mediated apoptosis and differentiation of K562 human erythroleukemia cells. Arch Biochem Biophys 1999;372:29–36. [PubMed: 10562413]
12. Sharma R, Brown D, Awasthi S, Yang Y, Sharma A, Patrick B, Saini MK, Singh SP, Zimniak P, Singh SV, Awasthi YC. Transfection with 4-hydroxynonenal-metabolizing glutathione S-transferase isozymes leads to phenotypic transformation and immortalization of adherent cells. Eur. J. Biochem 2004;271:1690–1701. [PubMed: 15096208]
13. Awasthi YC, Sharma R, Sharma A, Yadav S, Singhal SS, Chaudhary P, Awasthi S. Self-regulatory role of 4-hydroxynonenal in signaling for stress-induced programmed cell death. Free Radic Biol Med 2008;45:111–118. [PubMed: 18456001]
14. Yang Y, Sharma R, Cheng JZ, Saini MK, Ansari NH, Andley UP, Awasthi S, Awasthi YC. Protection of HLE B-3 cells against hydrogen peroxide- and naphthalene-induced lipid peroxidation and apoptosis by transfection with hGSTA1 and hGSTA2. Invest. Ophthalmol. Vis. Sci 2002;43:434–445. [PubMed: 11818388]

15. Yang Y, Cheng JZ, Singhal SS, Saini M, Pandya U, Awasthi S, Awasthi YC. Role of glutathione S-transferases in protection against lipid peroxidation: overexpression of hGSTA2-2 in K562 cells protects against hydrogen peroxide induced apoptosis and inhibits JNK and caspase 3 activation. J. Biol. Chem 2001;276:19220–19230. [PubMed: 11279091]
16. Yang Y, Sharma A, Sharma R, Patrick B, Singhal SS, Zimniak P, Awasthi S, Awasthi YC. Cells preconditioned with mild, transient UVA irradiation acquire resistance to oxidative stress and UVA-induced apoptosis: role of 4-hydroxynonenal in UVA-mediated signaling for apoptosis. J. Biol. Chem 2003;278:41380–41388. [PubMed: 12888579]
17. Sharma A, Patrick B, Li J, Sharma R, Jeyabal PVS, Reddy, Prasada MRV, Awasthi S, Awasthi YC. Glutathione S-transferases as antioxidant enzymes: Small cell lung cancer (H69) cells transfected with *hGSTA1* resist doxorubicin-induced apoptosis. Arch Biochem. Biophys 2006;452:165–173. [PubMed: 16890185]
18. Li J, Sharma R, Patrick B, Sharma A, Jeyabal PV, Reddy PM, Saini MK, Dwivedi S, Dhanani S, Ansari NH, Zimniak P, Awasthi S, Awasthi YC. Regulation of CD95 (Fas) expression and Fas-mediated apoptotic signaling in HLE B-3 cells by 4-hydroxynonenal. Biochemistry 2006;45:12253–12264. [PubMed: 17014078]
19. Sharma R, Sharma A, Dwivedi S, Zimniak P, Awasthi S, Awasthi YC. 4-Hydroxynonenal self-limits Fas-mediated DISC-independent apoptosis by promoting export of Daxx from the nucleus to the cytosol and its binding to Fas. Biochemistry 2008;47:143–156. [PubMed: 18069800]
20. Chen ZH, Saito Y, Yoshida Y, Sekine A, Noguchi N, Niki E. 4-Hydroxynonenal induces adaptive response and enhances PC12 cell tolerance primarily through induction of thioredoxin reductase 1 via activation of Nrf2. J. Biol. Chem 2005;280:41921–41927. [PubMed: 16219762]
21. Jacobs AT, Marnett LJ. HSF1-mediated BAG3 expression attenuates apoptosis in 4-hydroxynonenal-treated colon cancer cells via stabilization of anti-apoptotic Bcl-2 proteins. J. Biol Chem 2009;284:9176–9183. [PubMed: 19179333]
22. Jacobs AT, Marnett LJ. Heat shock factor 1 attenuates 4-Hydroxynonenal-mediated apoptosis: critical role for heat shock protein 70 induction and stabilization of Bcl-xL. J. Biol. Chem 2007;282:33412–33420. [PubMed: 17873279]
23. Zhao T, Singhal SS, Piper JT, Cheng J, Pandya U, Clark-Wronski J, Awasthi S, Awasthi YC. The role of human glutathione S-transferases hGSTA1-1 and hGSTA2-2 in protection against oxidative stress. Arch Biochem. Biophys 1999;367:216–224. [PubMed: 10395737]
24. Koeffler HP, Golde DW. Human myeloid leukemic cell lines: A Review. Blood 1980;56:344–350. [PubMed: 6996765]
25. Singhal SS, Saxena M, Ahmad H, Awasthi S, Haque AK, Awasthi YC. Glutathione S-transferases of human lung: characterization and evaluation of the protective role of the alpha-class isozymes against lipid peroxidation. Arch. Biochem. Biophys 1992;299:232–241. [PubMed: 1444461]
26. Habig WH, Pabst MJ, Jakoby WB. Glutathione S-transferases. The first enzymatic step in mercapturic acid formation. J. Biol. Chem 1974;249:7130–7139. [PubMed: 4436300]
27. Kolm RH, Danielson UH, Zhang Y, Talalay P, Mannervik B. Isothiocyanates as substrates for human glutathione transferases: structure-activity studies. Biochem. J 1995;311:453–459. [PubMed: 7487881]
28. Awasthi YC, Beutler E, Srivastava SK. Purification and properties of human erythrocyte glutathione peroxidase. J.Biol Chem 1975;250:5144–5149. [PubMed: 807573]
29. Carlberg I, Mannervik B. Glutathione reductase. Methods Enzymol 1985;113:484–490. [PubMed: 3003504]
30. Seelig GF, Meister A. Gamma-glutamylcysteine synthetase. Interactions of an essential sulfhydryl group. J. Biol. Chem 1984;259:3534–3538. [PubMed: 6142890]
31. Bradford MM. A rapid and sensitive method for the quantitation of microgram quantities of protein utilizing the principle of protein-dye binding. Anal. Biochem 1976;72:248–254. [PubMed: 942051]
32. Laemmli UK. Cleavage of structural proteins during the assembly of the head of bacteriophage T4. Nature 1970;227:680–685. [PubMed: 5432063]
33. Towbin H, Staehelin T, Gordon J. Electrophoretic transfer of proteins from polyacrylamide gels to nitrocellulose sheets: procedure and some applications. Proc. Natl. Acad. Sci. U S A 1979;76:4350–4354. [PubMed: 388439]

34. Englander EW, Hu Z, Sharma A, Lee HM, Wu ZH, Greeley GH. Rat MYH, a glycosylase for repair of oxidatively damaged DNA, has brain-specific isoforms that localize to neuronal mitochondria. J. Neurochem 2002;83:1471–1480. [PubMed: 12472901]
35. Mosmann T. Rapid colorimetric assay for cellular growth and survival: application to proliferation and cytotoxicity assays. J. Immunol Methods 1983;65:55–63. [PubMed: 6606682]
36. Beutler, E. Red Cell Metabolism. In: Grune; Stratton, editors. A Manual of Biochemical Methods. Orlando, FL: 1984.
37. Takizawa CG, Morgan DO. Control of mitosis by changes in the subcellular location of cyclin-B1-Cdk1 and Cdc25C. Current Opinion in Cell Biology 2000;12:658–665. [PubMed: 11063929]
38. Sánchez I, Dynlacht BD. New insights into cyclins, CDKs, and cell cycle control. Semin. Cell Dev Biol 2005;16:311–321. [PubMed: 15840440]
39. Kaufmann T, Schinzel A, Borner C. Bcl-w(edding) with mitochondria. Trends Cell Biol 2004;14:8–12. [PubMed: 14729175]
40. Ganju N, Eastman A. Bcl-X(L) and calyculin A prevent translocation of Bax to mitochondria during apoptosis. Biochem. Biophys. Res. Commun 2002;291:1258–1264. [PubMed: 11883953]
41. Candé C, Cohen I, Daugas E, Ravagnan L, Larochette N, Zamzami N, Kroemer G. Apoptosis-inducing factor (AIF): a novel caspase-independent death effector released from mitochondria. Biochimie 2002;84:215–222. [PubMed: 12022952]
42. Lorenzo HK, Susin SA, Penninger J, Kroemer G. Apoptosis inducing factor (AIF): a phylogenetically old, caspase-independent effector of cell death. Cell Death and Differ 1999;6:516–524.
43. Kwak MK, Itoh K, Yamamoto M, Sutter TR, Kensler TW. Role of transcription factor Nrf2 in the induction of hepatic phase 2 and antioxidative enzymes in vivo by the cancer chemoprotective agent, 3H-1, 2-dimethiole-3-thione. Mol Med 2001;7:135–145. [PubMed: 11471548]
44. Dinkova-Kostova AT, Holtzclaw WD, Cole RN, Itoh K, Wakabayashi N, Katoh Y, Yamamoto M, Talalay P. Direct evidence that sulfhydryl groups of Keap1 are the sensors regulating induction of phase 2 enzymes that protect against carcinogens and oxidants. Proc Natl Acad Sci U S A 2002;99:11908–11913. [PubMed: 12193649]
45. Nollen EA, Morimoto RI. Chaperoning signaling pathways: molecular chaperones as stress-sensing 'heat shock' proteins. J. Cell Sci 2002;115:2809–2816. [PubMed: 12082142]
46. Dai C, Whitesell L, Rogers AB, Lindquist S. Heat shock factor 1 is a powerful multifaceted modifier of carcinogenesis. Cell 2007;130:1005–1118. [PubMed: 17889646]
47. Salomoni P, Khelifi AF. Daxx: death or survival protein? Trends Cell Biol 2006;16:97–104. [PubMed: 16406523]
48. Esterbauer H, Schaur RJ, Zollner H. Chemistry and biochemistry of 4-hydroxynonenal, malonaldehyde and related aldehydes. Free Radic. Biol. Med 1991;11:81–128. [PubMed: 1937131]
49. Barrera G, Pizzimenti S, Muraca R, Barbiero G, Bonelli G, Baccino FM, Fazio VM, Dianzani MU. Effect of 4-Hydroxynonenal on cell cycle progression and expression of differentiation-associated antigens in HL-60 cells. Free Radic Biol Med 1996;20:455–462. [PubMed: 8720918]
50. Awasthi YC, Sharma R, Cheng JZ, Yang Y, Sharma A, Singhal SS, Awasthi S. Role of 4-hydroxynonenal in stress-mediated apoptosis signaling. Mol Aspects Med 2003;24:219–230. [PubMed: 12893000]
51. Jackson SJT, Singletary KW. Sulforaphane inhibits human MCF-7 mammary cancer cell mitotic progression and tubulin polymerization. J. Nutr 2004;134:2229–2236. [PubMed: 15333709]
52. Dashwood RH, Ho E. Dietary histone deacetylase inhibitors: from cells to mice to man. Semin Cancer Biol 2007;17:363–369. [PubMed: 17555985]
53. Joza N, Susin SA, Daugas E, Stanford WL, Cho SK, Li CY, Sasaki T, Elia AJ, Cheng HY, Ravagnan L, Ferri KF, Zamzami N, Wakeham A, Hakem R, Yoshida H, Kong YY, Mak TW, Zúñiga-Pflücker JC, Kroemer G, Penninger JM. Essential role of the mitochondrial apoptosis-inducing factor in programmed cell death. Nature 2001;410:549–554. [PubMed: 11279485]

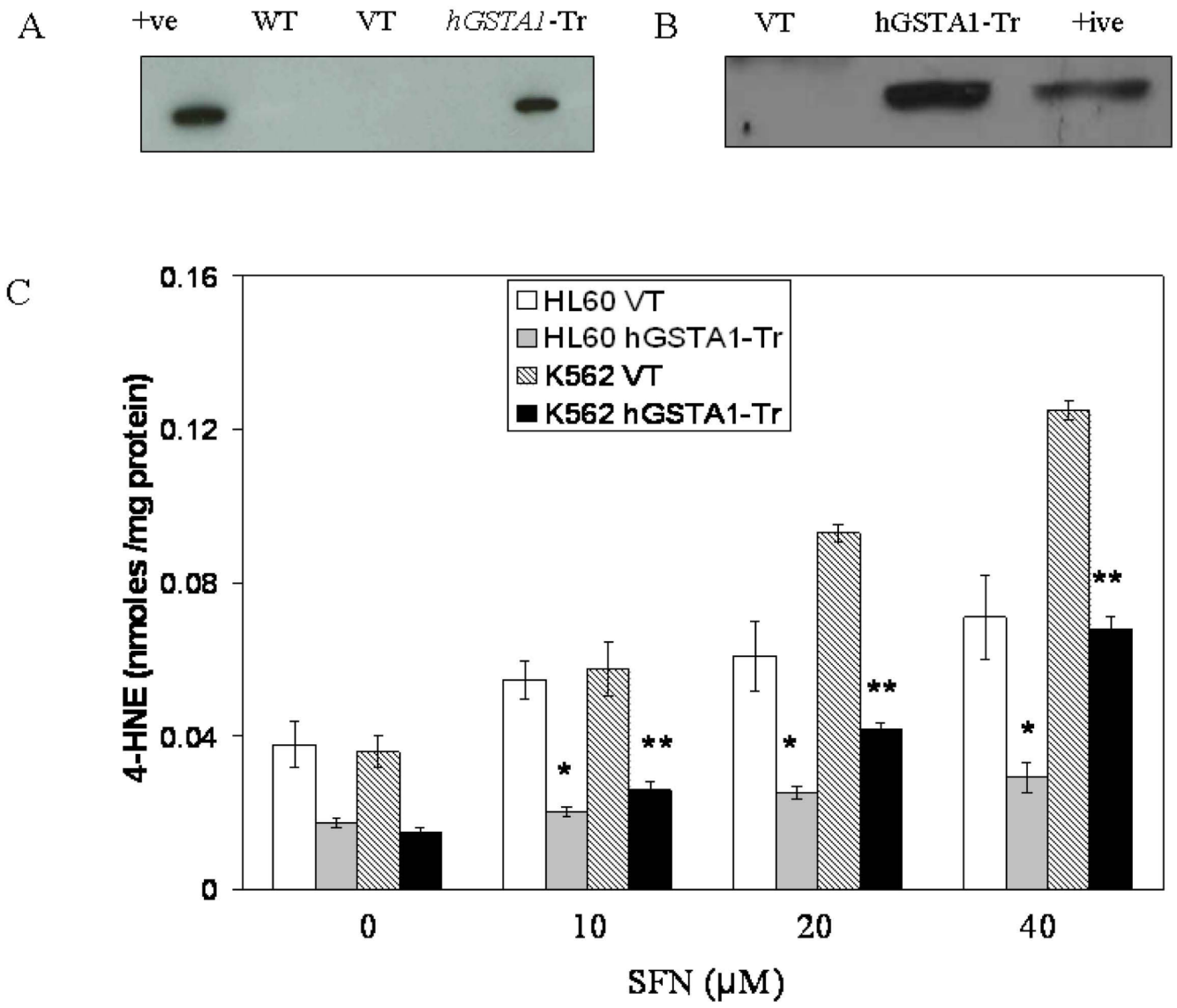

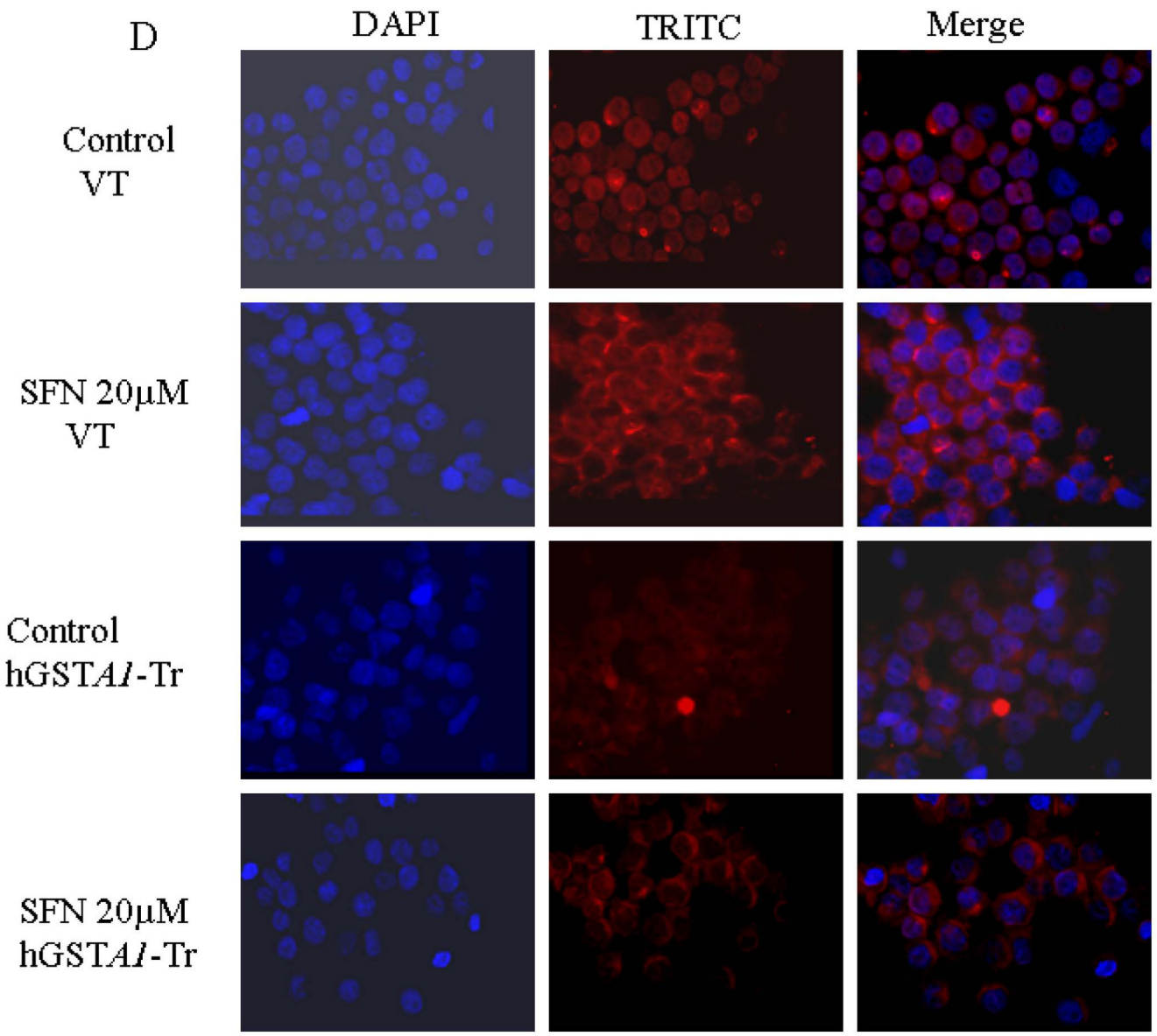

Fig. 1. Expression of hGSTA1-1 in *hGSTA1* transfected cells

HL60 (**A**) and K562 (**B**) cells were transfected with the cDNA of *hGSTA1* cloned in the pTarget-T mammalian expression vector or the vector alone as described in the Methods section. The supernatant fraction (28,000g) of homogenates of the wild-type (WT), vector (VT) and *hGSTA1*-transfected (*hGSTA1-Tr*) HL60 cells containing 30μg of protein was subjected to SDS-PAGE in 12% gel. Expression of hGSTA1-1 in the stable-transfected clone selected in G418 (300μg/ml) was analyzed by Western blot analysis using polyclonal primary antibodies against human α-class GSTs raised in rabbits and peroxidase-conjugated goat anti-rabbit secondary antibodies. The blot was developed using chemiluminescence (Supersignal West Pico, Pierce) reagents. Lanes have been appropriately marked on the immunoblots. Representative immunoblot from one of the several hGSTA1-1expressing clones selected is shown. **C. Levels of 4-HNE in SFN treated VT and hGSTA1-1 expressing HL60 and K562 cells**: VT and hGSTA1-1 expressing cells (2×10^7) were incubated with RPMI complete medium containing SFN (0–40μM) for 5h at 37°C. After pelleting them by centrifugation, cells

were washed and sonicated (3× 10s, 30W) in PBS containing BHT (5mM final concentration) on ice. 4-HNE levels in the cell pellets were measured by using LPO-586 kit as per the manufacturer's instructions. Data presented are Mean ± SD (n=3, * and ** represent a significant difference in 4-HNE levels of VT and hGSTA1-1 expressing HL60 and K562 cells respectively; $p < 0.05$). **D. Immunofluorescence analysis of 4-HNE adducts in SFN treated VT and hGSTA1-1 expressing HL60 cells**: VT and hGSTA1-1 expressing HL60 cells (1×10^6) were treated with SFN (20μM) for 2h at 37°C in RPMI complete medium. After pelleting them by centrifugation at 1000rpm (5min), cells were washed and resuspended in PBS. Aliquots of cell suspensions were cytospun at 500rpm for 5 min onto the superfrost Fisher brand slides and fixed in 4% paraformaldehyde for 20min. The cells were incubated with the primary antibodies against 4-HNE-protein adduct (1:500) prepared in the blocking buffer (1% BSA +1% goat serum in PBS) overnight at 4°C in a humidified chamber. After three washings with PBS (5min each), cells were incubated with TRITC conjugated secondary antibodies (1:500) for 2h at room temperature. Subsequently, this was once again followed by three washings with PBS (10min each), mounted with Vecta Shield containing DAPI and observed under the Nikon Eclipse E800 fluorescence microscope with a 40x objective. Different panels of photographs with DAPI and TRITC stains have been appropriately marked in the figure.

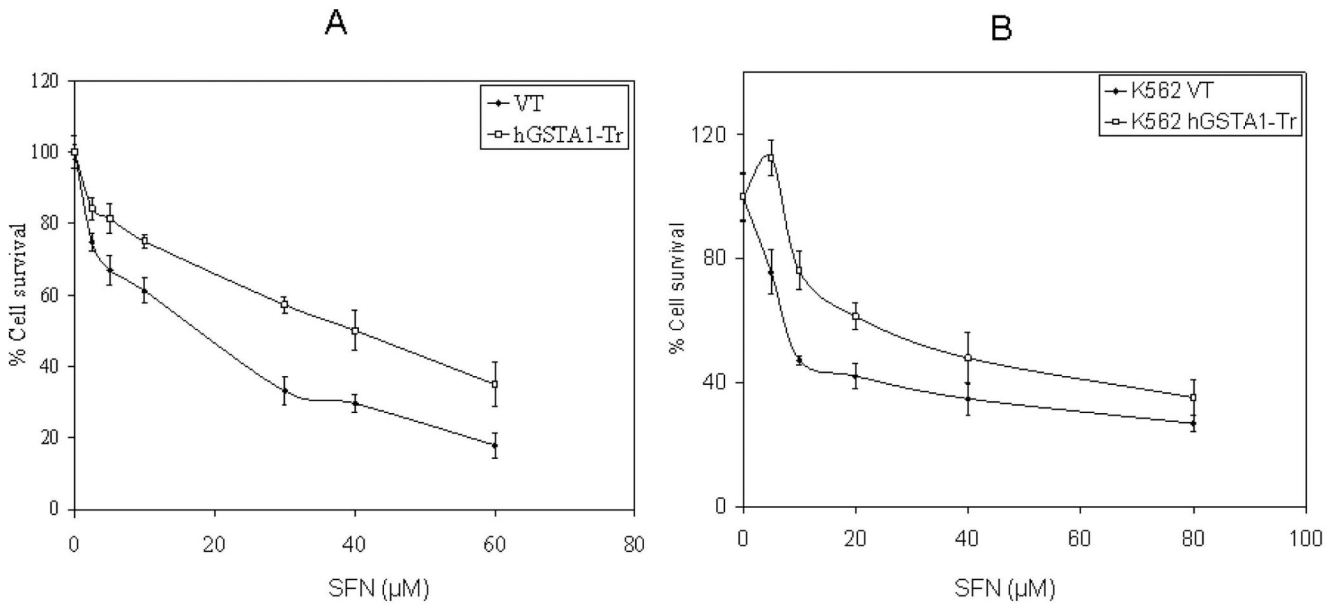

Fig. 2. Cytotoxic effects of SFN on VT and hGSTA1-1 expressing cells

VT and hGSTA1-1 expressing HL60 (**A**) and K562 (**B**) cells (2×10^4) were plated into replicate wells of a 96 well plate in RPMI complete growth medium. After incubating the cells overnight, cells were treated with different concentrations of SFN (0–60μM) prepared in DMSO (final concentration; 0.02%) with appropriate controls and were incubated for 24h at 37 °C after which the MTT assay was performed as described in the Materials and Methods section. The OD_{580} values of samples subtracted from those of respective blanks (no cells) were normalized with control values. The values shown are Mean ± SD (n=3 done in quadruplets, $p<0.01$).

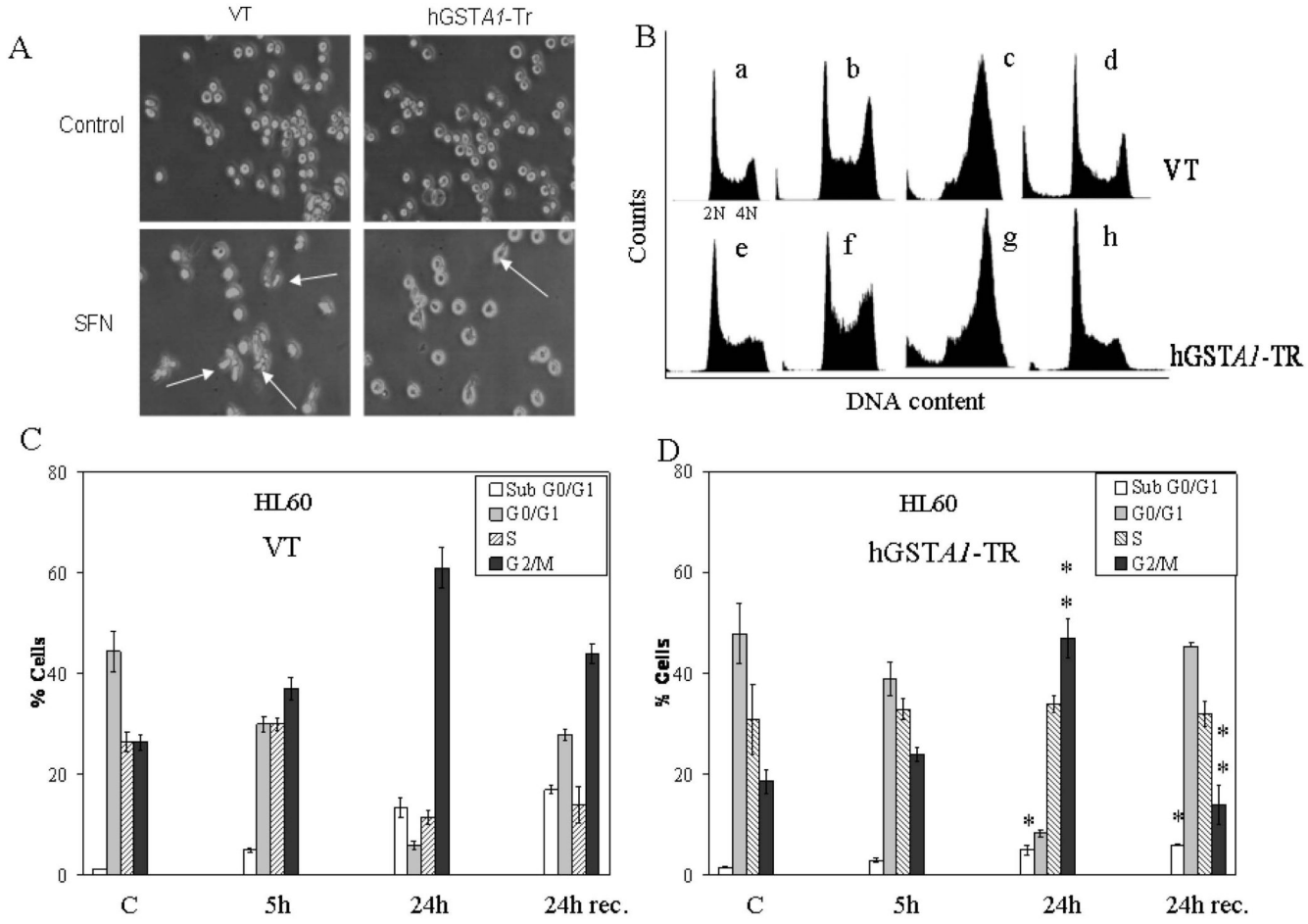

E

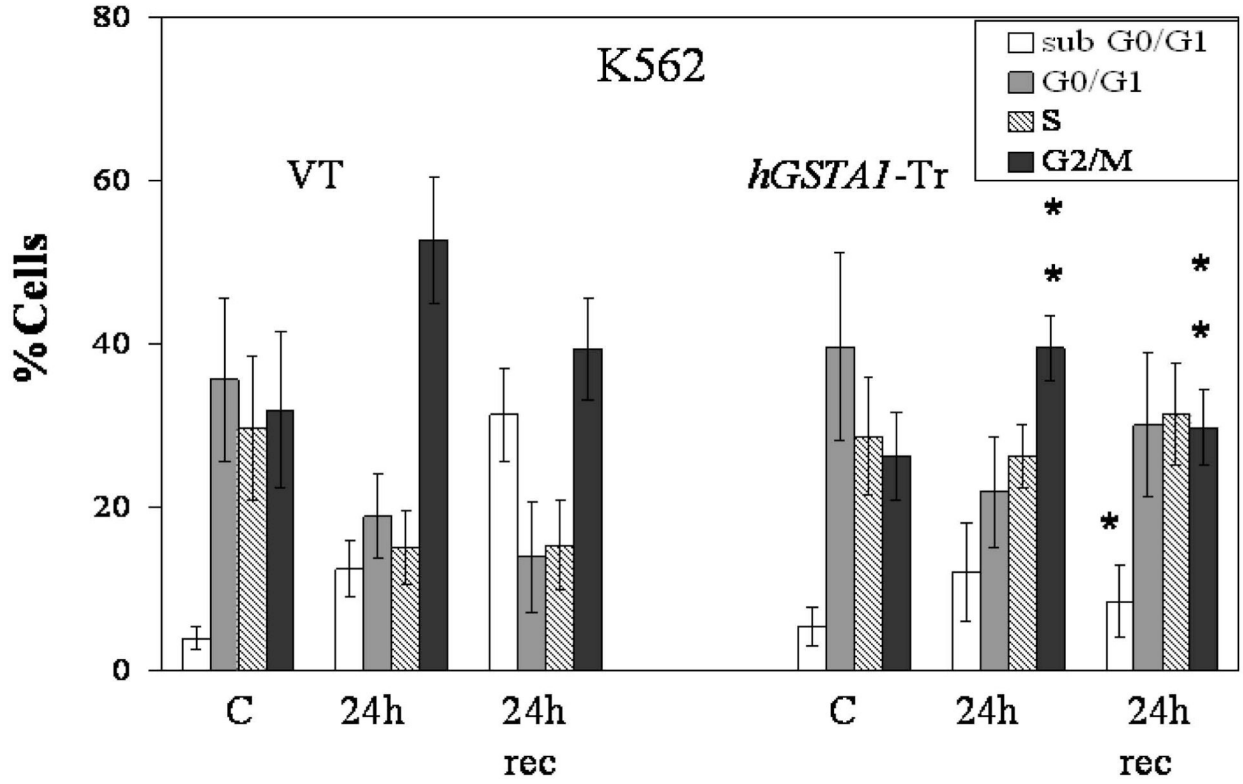

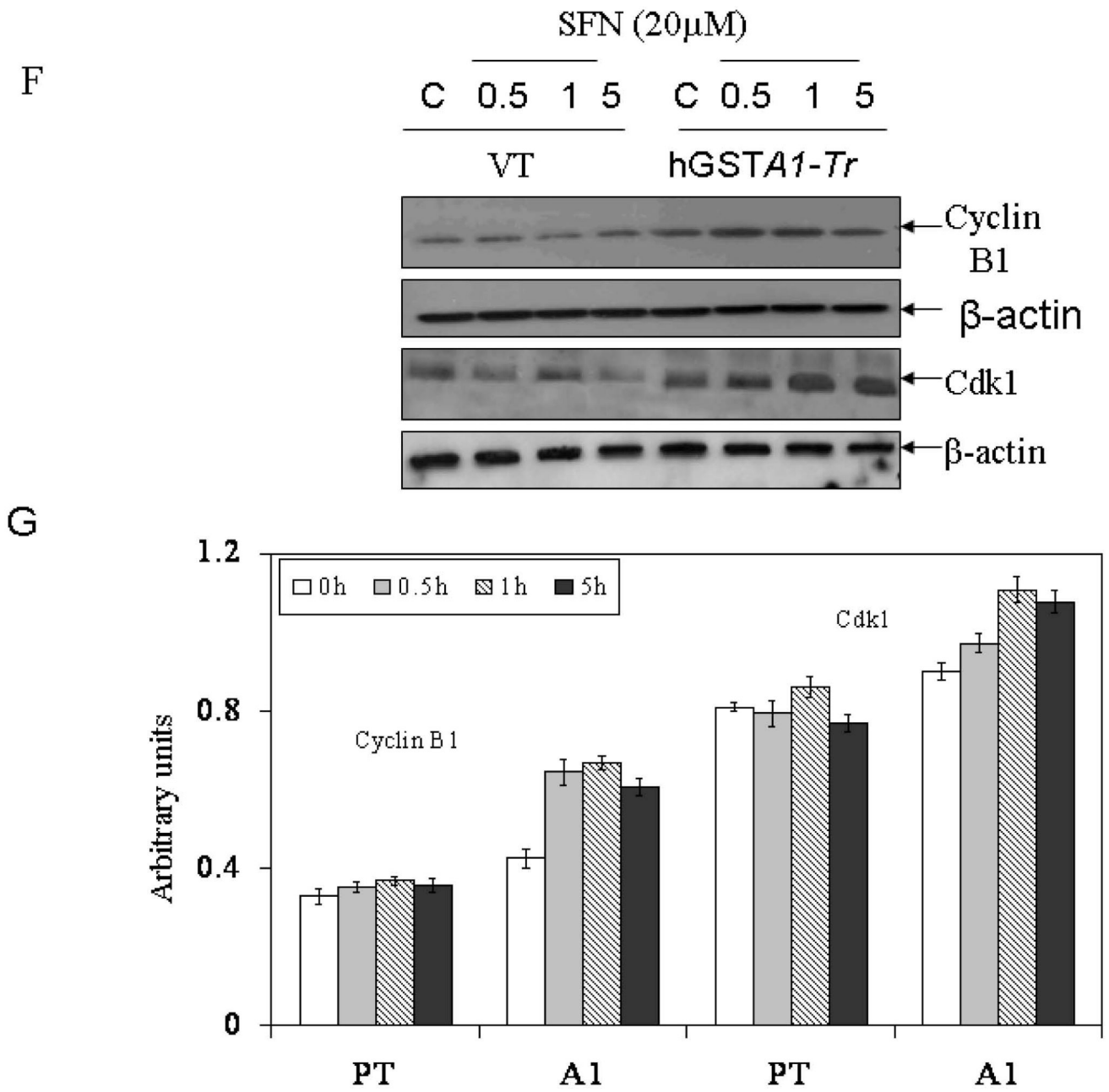

Fig. 3. FACS analysis of the SFN-induced cell cycle arrest in VT and hGSTA1-1 over expressing cells

Cells (2×10^5) plated in complete growth medium were treated with SFN (20μM) for 5h and 24h time points at 37°C with appropriate controls. Separate groups of cells were also allowed to recover for 24h after a 24h treatment of SFN. After the treatment, cells were pelleted, washed with PBS and fixed in an ice cold 70% ethanol. As described in the Methods section, cells were stained with propidium iodide (1mg/ml) and analysed using the Beckman Coulter Cytomics FC500, Flow Cytometry Analyzer. **A**. Morphology of cells undergoing SFN induced cell cycle arrest (shown by arrows) viewed under a phase contrast light microscope **B**. Flow cytometric histograms of the percentage of cells in different phases of cell cycle (a–d; (upper) VT and e–f; (lower) *hGSTA1*-transfected cells) Panel a &e: control; b&f: 5h SFN treatment c&g: 24h

SFN treatment d&h: 24h recovered cells after 24h of SFN treatment. **C** and **D**, Bar charts showing the percentage of cells in the respective phases (sub G0/G1, G0/G1, S and G2/M) of the cell cycle (Mean ± SD) from three independent experiments. **E**. Bar chart showing the effect of SFN on the cell cycle of K562 (VT and *hGSTA1* transfected) cells. **F** Western blot analysis of cell cycle related proteins Cdk1 and cyclin B1expression respectively in control and SFN treated VT and hGSTA1-1 expressing HL60 cells. G. Densitometric analysis of bands obtained for cyclin B1 and cdk1 on immunoblots.* and **represent significant differences in the percentages of cells in apoptosis (sub G0/G1) and G2/M Phase respectively in VT and hGSTA1-1.

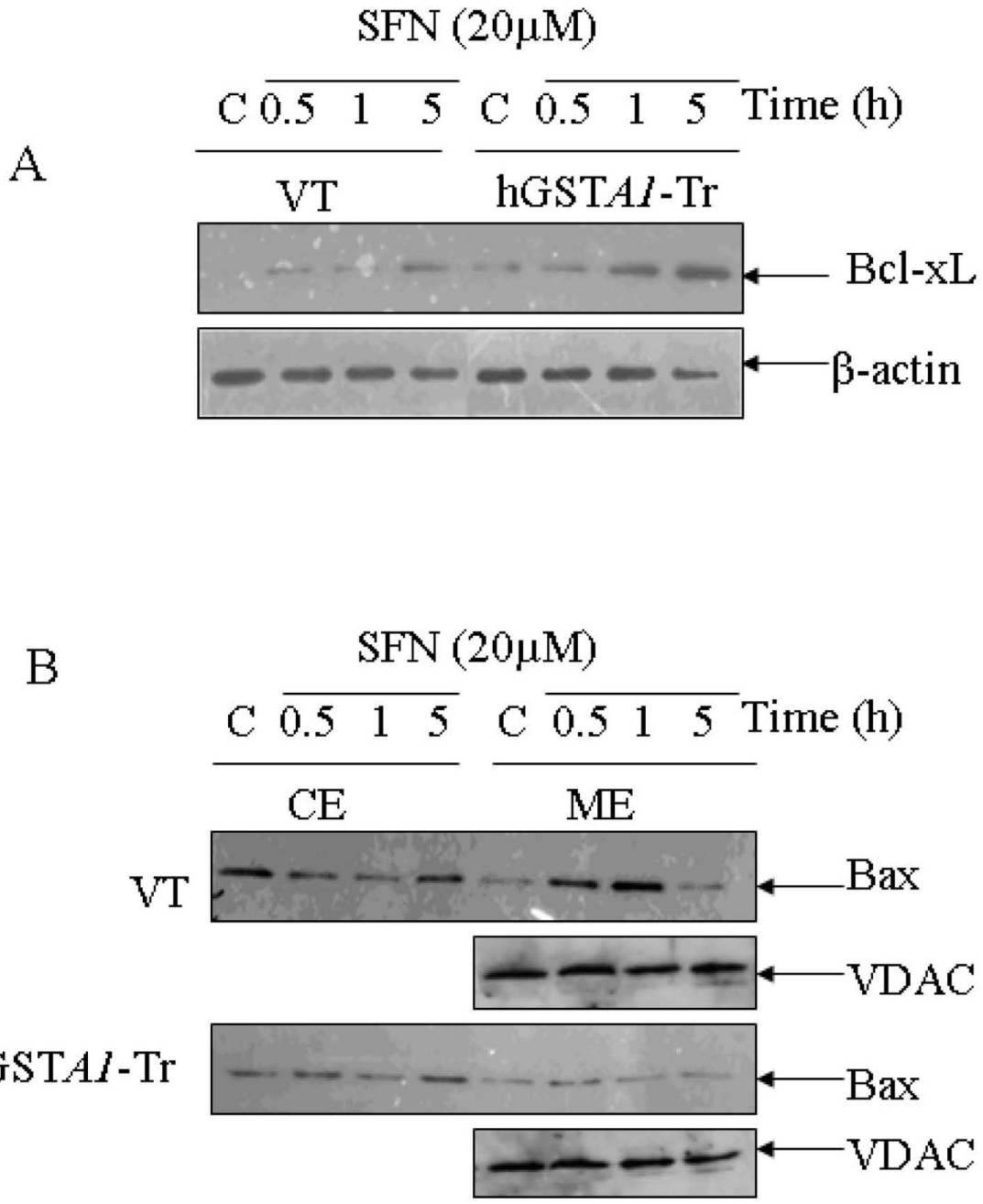

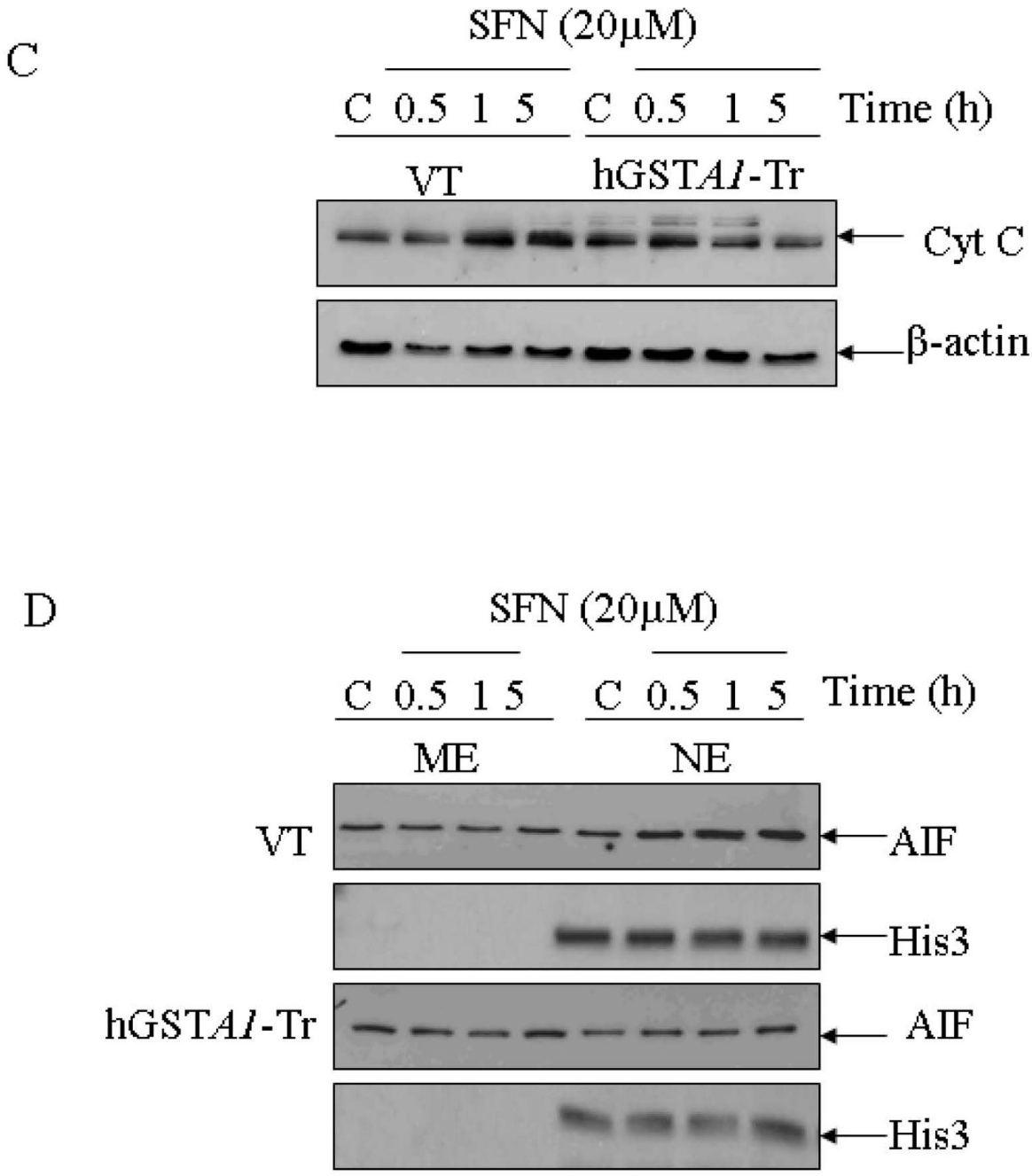

Fig. 4. Effects of SFN on the expression of apoptosis related proteins (Bcl-xL, Bax, AIF and cytochrome C) in VT and hGSTA1-1 expressing HL60 cells

Plated cells (5×10^6) were incubated with SFN (20μM) in complete RPMI growth medium for different time points (0.5h, 1h and 5h) at 37°C. After treatment, they were pelleted by centrifugation and washed 2X with PBS. Whole cell extracts were prepared in RIPA lysis buffer while sub cellular (cytoplasmic, nuclear and mitochondrial) fractionation was performed as described in Materials and Methods and by the Imgenex Kit as per the manufacturer's instructions. Western blot analyses of these extracts were carried out by using antibodies against Bcl-xL (panel **A**), Bax (panel **B**); cytochrome C (panel **C**) and AIF (panel **D**). Immunoblots were also probed with β-actin (total and cytoplasmic extracts to ascertain equal

loading of proteins. The blot was developed using chemiluminescence (Supersignal West Pico, Pierce) reagents to detect the bands on immunoblots.

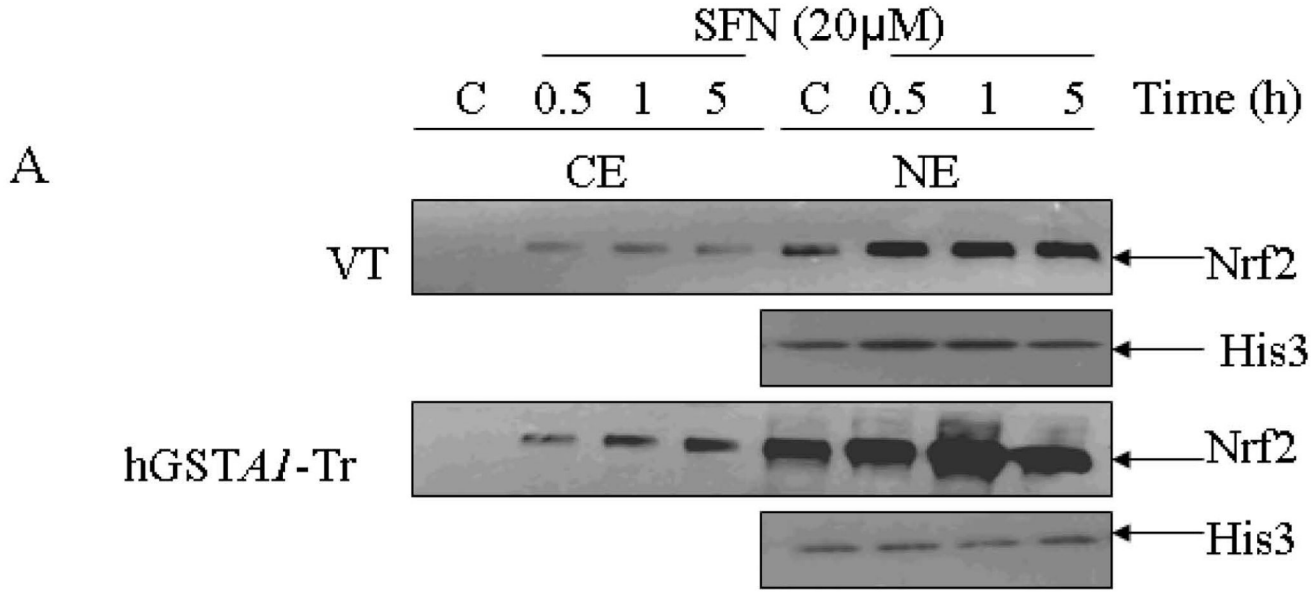

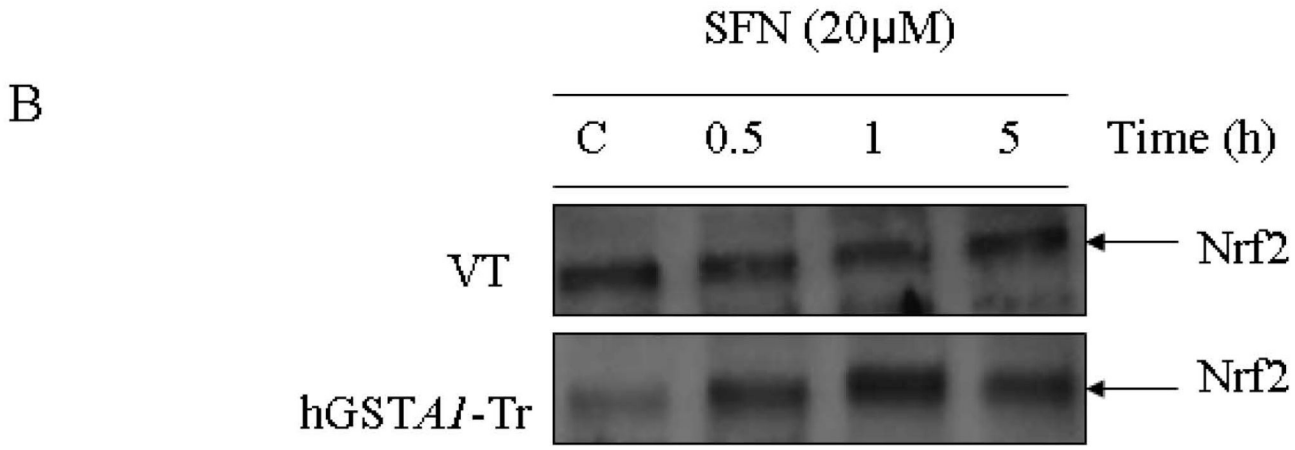

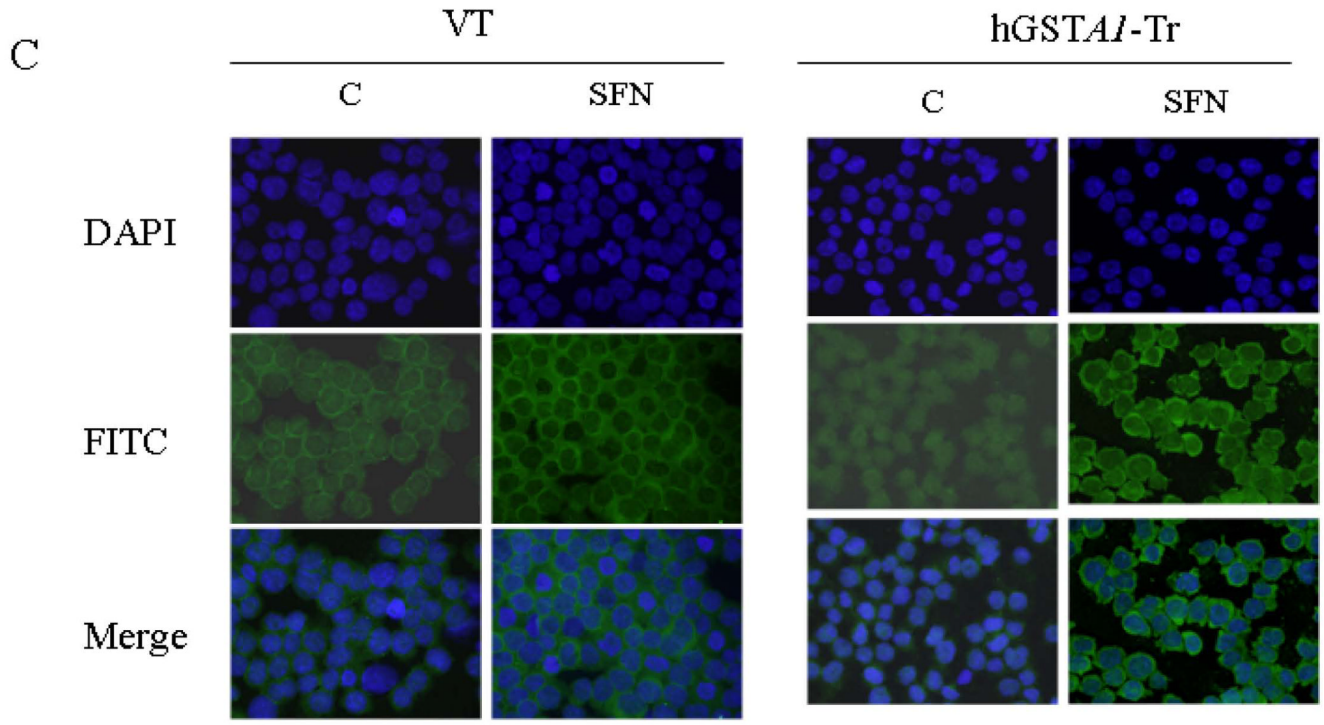

Fig. 5. A. Effect of SFN on the expression and localization of Nrf2 in VT and hGSTA1-1 expressing cells

Cells were treated with SFN (20μM) for different time points (0.5, 1 and 5h). Cytoplasmic and nuclear extracts of control and treated cells were prepared and subjected to Western blot analyses as described in the legend of Fig. 4. A representative Western blot showing the expression of Nrf2 in cytoplasmic and nuclear protein fractions obtained from control and SFN treated VT and **hGSTA1-1 expressing** HL60 cells. **B**. Western blot of nuclear extract of VT and **hGSTA1-1 expressing** K562 cells. **C. Immunofluorescence localization of Nrf2 in control and SFN treated VT and hGSTA1-1 expressing HL60 cells**. Control and SFN treated cells (2×10^5) for immunolocalization of Nrf2 were essentially processed as described in the legend for Fig. 2B except that antibodies used were those against Nrf2 (diluted 1:200 in blocking buffer) and FITC conjugated secondary antibodies.

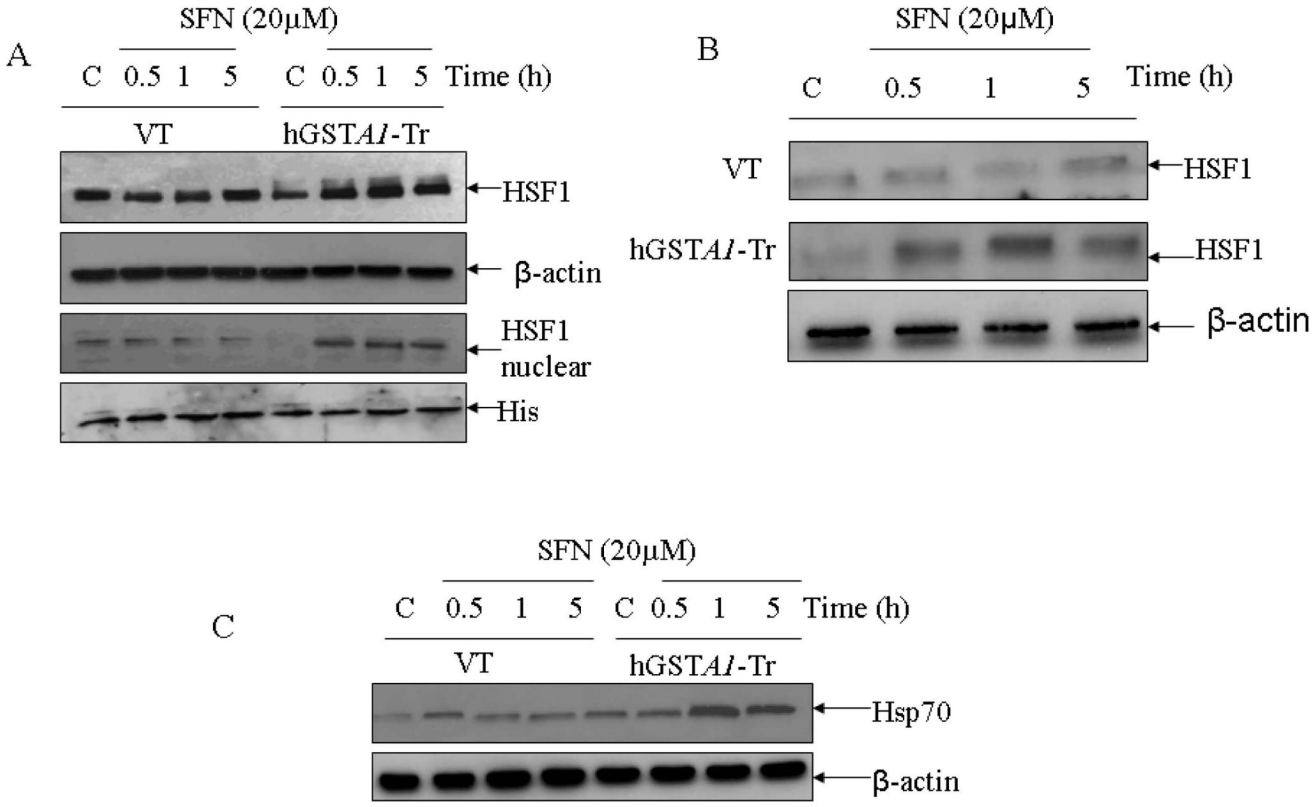

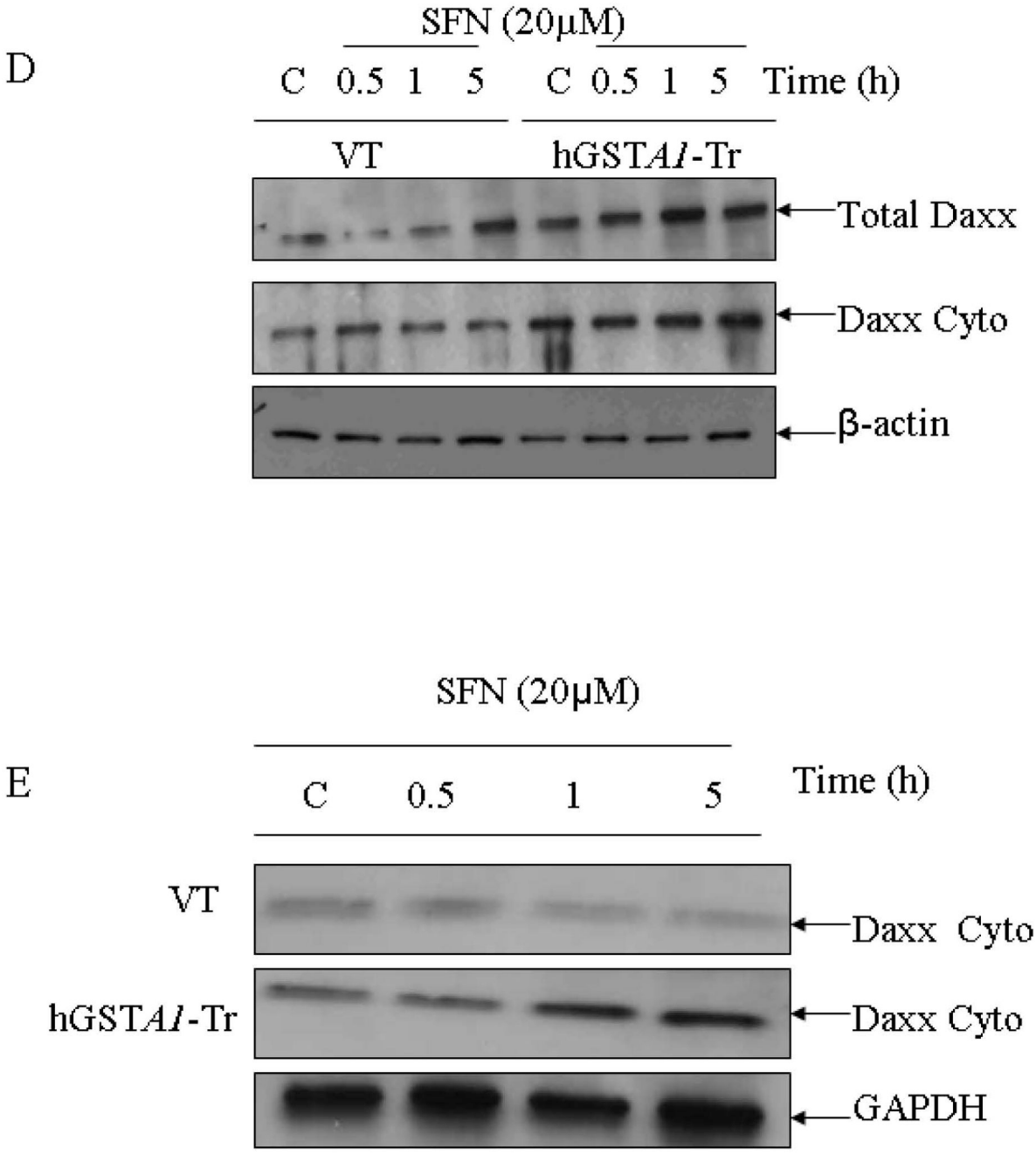

Fig. 6. Effect of SFN on the expression and localization of HSF1 (A and B), Hsp70 (C) and Daxx (D and E) in VT and hGSTA1-1 expressing cells

Cells (2×10^6) were treated with SFN (20μM) in complete growth medium at 37°C for different time points as shown in the figure. Total cell extracts in RIPA buffer, cytoplasmic and nuclear fractions of the cells were prepared as described in the Method section. Western blot analyses of the SDS-PAGE resolved proteins (50–60μg protein in each lane) were carried out by using antibodies against Daxx, HSF1, and Hsp70 as described in the Methods section.

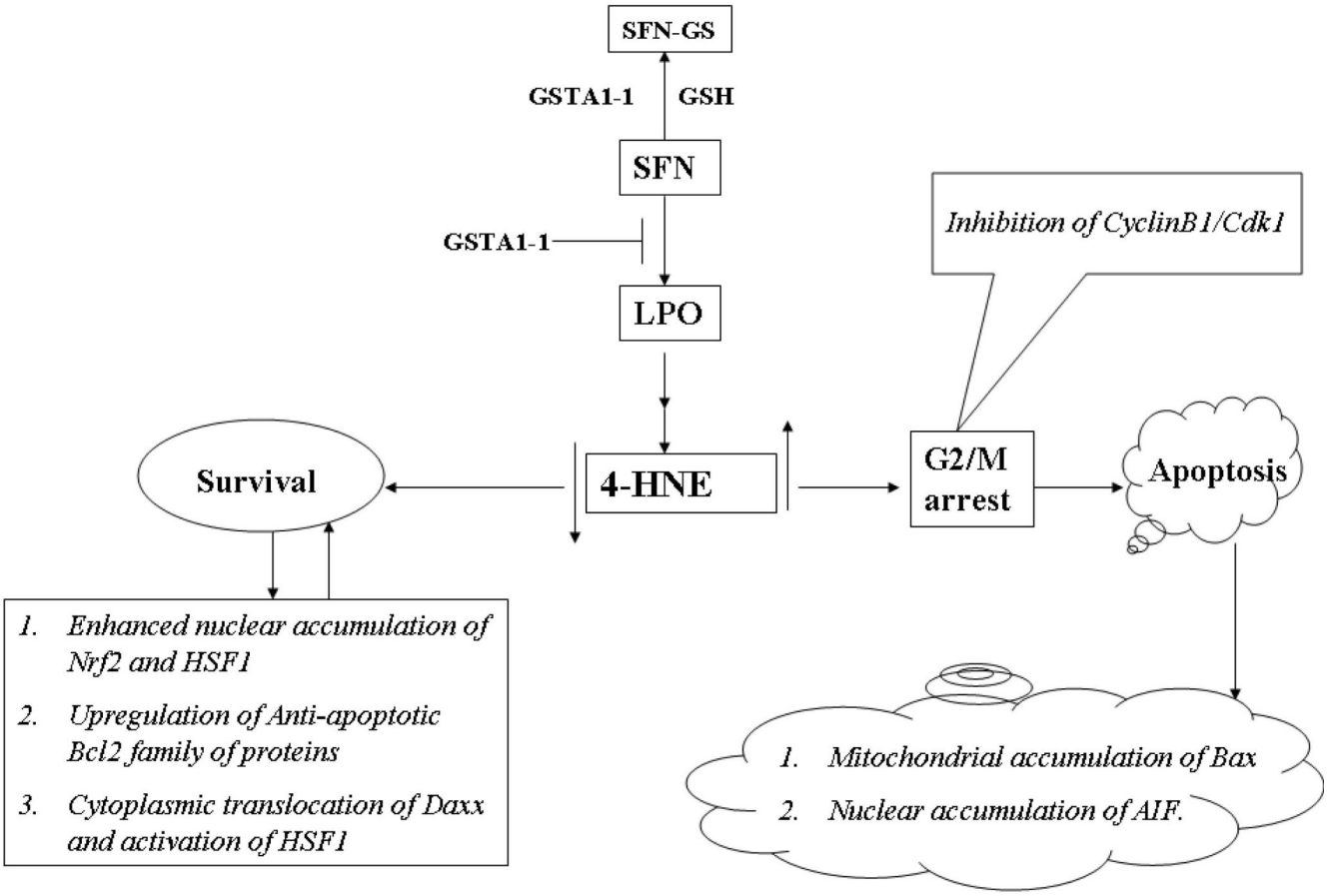

Fig. 7. A theoretical model for the mechanisms by which SFN-induced generation and accumulation of 4-HNE affects signaling for cell cycle arrest and apoptosis and inhibition of these effects of SFN by GSTA1-1

The model illustrates that treatment of cells with SFN causes enhanced LPO-induced accumulation of 4-HNE which contributes to SFN-induced cell cycle arrest in G2/M phase through inhibition of cyclin B1 and cdk1, and apoptosis via down regulation of anti-apoptotic Bcl-xL, increased translocation of proapototic Bax to mitochondria, increased accumulation of AIF to nucleus and cytoplasmic release of cytochrome C. These SFN-induced effects are inhibited by the enforced expression of GSTA1-1 in cells. The over expression of GSTA1-1 limits the formation of 4-HNE by reducing upstream LPO products, which leads to the up regulation of Bcl-xL, facilitated cytoplasmic export of the transcription repressor Daxx accompanied by enhanced nuclear accumulation of the transcription factors Nrf2 and HSF1, and activation of the associated stress responsive antioxidant and heat shock proteins.

Table 1

Specific activities of antioxidant enzymes in empty vector (VT) and *hGSTA1*-transfected HL60 cells

S.No.	Enzyme	Specific activity (nmol/min/mg protein, Mean ± SD, n=3)	
		VT	hGST*A1*-Tr
1	**GSTs**		
	*CDNB	66.38 ± 2.7	121.7 ± 4.6
	*SFN	92.0 ± 6.4	170 ± 11
2	**GPx**		
	**CU-OOH	0.175 ± 0.034	0.788 ± 0.12
3	**GR**	36 ± 2.4	43 ± 1.82
4	**γGCS**	44.4 ± 3.67	80.13 ± 4.48

*Substrates of GSTs

**Substrate of GPx

The activities of GSTs against 1-chloro-2, 4-dinitrobenzene (CDNB) (26) and sulforaphane (SFN) (27) were measured in the crude cytosolic extracts (28000g supernatants) prepared from the empty vector and hGSTA1-transfected cells. GPx activity against cumene hydroperoxide (CU-OOH) (27), activities of GR (28) and γGCS (29) were also estimated in the crude extracts.